FUTURE MEDICINAL CHEMISTRY
2025, VOL. 17, NO. 5, 557–573
https://doi.org/10.1080/17568919.2025.2470110

Taylor & Francis
Taylor & Francis Group

RESEARCH ARTICLE

OPEN ACCESS Check for updates

Synthesis and in vitro antitrypanosomatid activity of novel 5-nitroindole-rhodanine conjugates

Emce Badenhorst [a], Janine Aucamp [a], Christina Kannigadu [a], Helena D. Janse van Rensburg [a], Keisuke Suganuma [b] and David D. N'Da [a]

[a]Centre of Excellence for Pharmaceutical Sciences, North-West University, Potchefstroom, South Africa; [b]National Research Center for Protozoan Diseases, Obihiro University of Agriculture and Veterinary Medicine, Obihiro, Japan

ABSTRACT

Aim: Trypanosomatid diseases, leishmaniasis and trypanosomiasis are vector-borne parasitic diseases that can cause death and catastrophic economic losses for millions of people. The growing resistance of trypanosomatid parasites to current treatments highlights the urgent need for new therapeutic agents. This study explored 5-nitroindole-rhodanine conjugates to identify promising new compounds with the potential for future development as antitrypanosomatid treatments.

Materials and methods: The conjugates were synthesized in a multi-step process and evaluated *in vitro* for antileishmanial activity against Leishmania (*L.*) *donovani* and *L. major* strains. Cytotoxicity was assessed on Vero and THP-1 cells. Due to the taxonomic relation to Trypanosoma spp. the compounds were also screened for in vitro activity against species that cause zoonotic trypanosomiasis.

Results and conclusion: Several hits were found with leishmanicidal activity against both *L. donovani* and *L. major* strains. Of these, **3d** was identified as a potential early lead that exhibited nanomolar cidal activity against *L. major*, and greater selectivity than the reference drug amphotericin B. However, the compounds did not have similar activity levels against *Trypanosoma spp*. Hence, these compounds should be further investigated for their mechanism of action and *in vivo* antileishmanial activity to determine their potential as a leishmaniasis treatment.

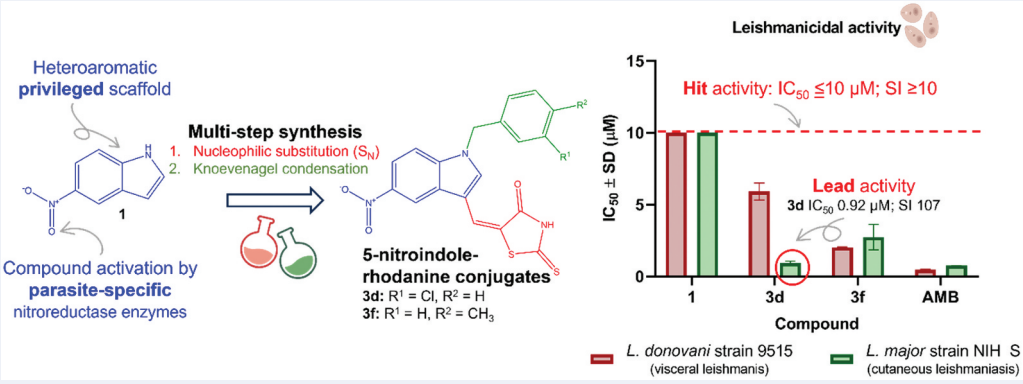

ARTICLE HISTORY
Received 28 November 2024
Accepted 17 February 2025

KEYWORDS
Cytotoxicity; leishmaniasis; molecular hybridization; nitroindole; rhodamine

1. Introduction

Leishmaniasis is a communicable disease caused by over 20 species of protozoan parasites from the genus *Leishmania*, which are spread to humans through the bite of an infected female sandfly [1]. This disease is prevalent in the east Mediterranean area, South America, East Africa, and the Indian subcontinent [2,3]. A significant number of people are affected in these subtropical and tropical regions, with 6.21 million cases reported worldwide and an additional 1.1 million cases occurring annually.

Leishmania infects phagocytic cells of the immune system, causing immunopathology that can manifest as various diseases [4,5]. Cutaneous leishmaniasis (CL), the most prevalent disease manifestation, presents as disfiguring and stigmatizing skin lesions and permanent scars [6]. Mucocutaneous leishmaniasis (MCL) is a rare disease manifestation that presents as destructive lesions of the mucosal membranes of the nose, mouth, and throat [7]. Visceral leishmaniasis (VL) presents as a systemic infection that can result in wasting, liver dysfunction, renal impairment, blood dyscrasias, recurrent bacterial

CONTACT David D. N'Da david.nda@nwu.ac.za Centre of Excellence for Pharmaceutical Sciences, North-West University, Potchefstroom Campus, 11 Hoffman Street, Private Bag X6001, Potchefstroom 2520, South Africa

Supplemental data for this article can be accessed online at https://doi.org/10.1080/17568919.2025.2470110

Article highlights

- A series of seventeen novel 5-nitroindole derivatives, including twelve conjugates tethering 5-nitroindole and rhodanine synthons, were synthesized in poor to excellent yields (25–93%) through a multi-step process.
- *In silico* pharmacokinetic properties calculated on SwissADME suggested derivatives **2b**, **3a**, and **4b** as potential orally bioavailable hits/leads.
- The general cytotoxic activities of the derivatives were evaluated against normal mammalian Vero (African green monkey kidney epithelial) and Madin-Darby bovine kidney (MDBK) cells. In contrast, host THP-1 (human acute monocytic leukemia) cells were used to assess macrophage-specific toxicity. The resazurin assay for Vero and THP-1 and the Cell Counting Kit-8 solution (CCK-8) for MDBK cells were used, respectively.
- The antileishmanial activity of the compounds was evaluated against *L. major* strain NIH S and antimony-resistant *L. donovani* strain 9515, the causative agents of cutaneous leishmaniasis (CL) and the potentially lethal visceral leishmaniasis (VL), respectively.
- The antitrypanosomal activity of the derivatives was assessed against an array of *Trypanosoma* (*T.*) strains, including human African trypanosomiasis (HAT) subspecies *T. brucei* (*b.*) *gambiense* IL1922 and *T. b. rhodesiense* strain IL1501, as well as animal trypanosomiasis (AT) subspecies *T. b. brucei* GUTat3.1, *T. congolense* IL3000 and *T. equiperdum* IVM-t1 using Cell-TiterGlo reagent.
- The compounds displayed moderate to low toxicity to Vero, MDBK, and THP-1 cells.
- Potent and selective hits and a potential early lead were identified against *L. donovani* strain 9515 and *L. major* strain NIH S, with the cellular potency IC_{50}'s varying from 0.5 to 10 µM.
- Conjugate **3f** was the most active against *L. donovani*, with hit-like and leishmanicidal activity (IC_{50} 2.02 µM; SI 11) and *in silico* predicted oral bioavailability.
- Derivative **3d** was the most potent against *L. major*, with lead-like and leishmanicidal activity (IC_{50} 0.92 µM; SI > 107) and *in silico* predicted oral bioavailability.
- No significant antitrypanosomal activity was uncovered.
- Both **3d** and **3f** conjugates stood as promising candidates for further *in vivo* antileishmanial testing.

infections, and death [8]. Leishmaniasis negatively impacts not only the physical health of persons infected but also their mental, social [9] and economic well-being [10]. As of November 2024, 53 VL-endemic countries (66%) and 56 CL-endemic countries (62%) reported data to the World Health Organization (WHO) Global Leishmaniasis Program for 2023 [1]. In 2023, about 83% of global VL cases were reported from seven countries, including Brazil, Ethiopia, India, Kenya, Somalia, South Sudan, and Sudan. Furthermore, six countries reported more than 5000 CL cases, namely Afghanistan, Algeria, Brazil, Pakistan, Peru and the Syrian Arab Republic, accounting for 83% of global reported CL incidence [1].

Leishmaniasis is a neglected tropical disease (NTD) that affects mostly poor people in tropical areas of the world [1]. These people are especially vulnerable to these diseases and their detrimental effects, due to association with malnutrition, immunodeficiency, and lack of resources. Unfortunately, despite their significance, the NTDs have historically received little attention in the global health agenda [11]. Accordingly, preventative, diagnostic, and therapeutic measures are fraught with issues [12,13].

The present treatment of leishmaniasis comprises mainly a handful of drugs, including pentavalent antimonials, amphotericin B (AMB), miltefosine, paromomycin, and pentamidine [14]. These drugs are not optimal as they have varied efficacy and toxicity, are expensive, and require mostly parenteral administration for extended durations in a hospital [14,15]. Patients lack adherence to these inconvenient treatments, which may exacerbate the emerging problem of drug resistance, which most of these treatments are vulnerable to [15,16]. New, effective, and safe antileishmanial therapeutics are critically needed to combat the risk of the disease's future unresponsiveness to current drugs.

Furthermore, *Leishmania* shares taxonomic, biological, and epidemiologic similarities or overlaps with *Trypanosoma* (*T.*), the causative species for zoonotic trypanosomiases [17]. Progression in advancing antileishmanial drug discovery may be of similar benefit for managing trypanosomiases [18]. Human African trypanosomiasis (HAT) is currently well managed, with the elimination of the chronic (*T. brucei gambiense*-related) HAT expected by 2030 [19]. However, elimination seems impossible for the acute (*T. b. rhodesiense*-related) HAT due to its zoonotic nature and large animal reservoir. Animal trypanosomiasis (AT) mainly occurs as a wasting disease (nagana, dourine, surra) in domesticated and wild animals [20]. These diseases remain widespread, with no significant improvement in burden reported within the past two decades [20]. This causes millions of deaths per annum and results in a substantial collective health and economic impact [21].

Privileged scaffolds are molecular frameworks that have a significant therapeutic potential [22]. Compounds containing these scaffolds were shown to be prolific among bioactive substances. Privileged scaffolds have structural features that enable interaction with several biomolecular receptors. More than promiscuous receptor binders, they have a simplicity of optimization and, with appropriate synthetic modification, may provide valuable ligands for various biomolecular receptors [23]. Therefore, privileged scaffolds serve as valuable starting points for drug discovery, allowing for the rapid identification of hit compounds.

Indole is a heteroaromatic privileged scaffold with a pyrrole ring fused to a benzene ring [24]. It can participate in a range of supramolecular interactions due to its nucleophilic aromatic structure. Furthermore, the presence of an acidic N-H facilitates its favorable interaction with various biomolecular receptors [23]. Indole also has extraordinary synthetic accessibility [25]. Therefore, over 10 000 bioactive indole derivatives exist, including over 200 diverse drugs that are either clinical candidates or on the pharmaceutical market [26]. Indole derivatives have a wide range of therapeutic applications, including infectious diseases [27], cancer [28], inflammatory diseases [29], hypertension [30], depression [31], and diabetes [32]. It is thus unsurprising that many indole derivatives were also found to have *in vitro* antileishmanial and antitrypanosomal activities, with generally good cytotoxicity profiles. A few examples include bisindoles [33], indole-pyrazolopyridines [34], *gem*-dithioacetylated indoles [35], indole-thiosemicarbazones [36], thiazolidinone/phenylindole hybrids [37], N5-substituted paullones [38], indole bichalcophenes [39], and phenylindoles [40].

Rhodanine is a five-membered heterocyclic compound also regarded as a privileged scaffold [41], consisting of carbonyl, thiocarbonyl, thioether, amino, and methylene groups. This synthon can bind to multiple biomolecular receptors, enabled by the high density of polar intermolecular interactions that

may occur on the scaffold. The thiocarbonyl group and the presence of an exocyclic double bond on the methylene carbon (5-ene-rhodanine) are critical for the multi-target affinity of the scaffold [42]. Accordingly, rhodanine, especially 5-ene-rhodanine [43], has a multitude of bioactivities, including antibacterial [44], antiparasitic [45], antiviral [46], antidiabetic [47], anti-tumor [48], anti-inflammatory [49], as well as *in vitro* antileishmanial [37] and antitrypanosomal [50] potential. However, the reactivity of rhodanine, especially its 5-ene bond, is controversially linked to toxicity, though this claim has never been proved or refuted [41]. As such, the cytotoxicity of rhodanine should be carefully evaluated. Of note, rhodanine is synthetically accessible and thus valuable for the drug discovery process [41].

The nitro group may contribute to a compound's bioactivity by directly interacting with biomolecules and/or forming reactive electrophilic regions within the compound due to its electron-withdrawing capabilities [51]. Moreover, nitroreductase enzymes (NTRs) can metabolize nitro to form reactive oxygen and nitrogen species (RONS), which may react with and damage various biomolecules [52]. This cytotoxicity of nitro has been extensively utilized and investigated in treating infectious diseases. However, inappropriate activation of the nitro group by human NTRs might result in substantial side effects [51]. Compound activation by NTRs present in *Leishmania* and *Trypanosoma* (NTR1 and NTR2) that are absent from human cells can potentially cause selective toxicity to the parasite [53,54]. Several nitroaromatic compounds were found to be effective *in vivo* against CL, VL, and HAT, including the antitrypanosomal 5-nitroimidazole fexinidazole [55], the 6-nitro-imidazooxazoles delamanid [56] and DNDI-VL-2098, and the 2-nitro-imidazooxazines DNDI-0690, trypanocide DNDI-8219 [57], and analogues of (*R*)-pretomanid [58,59]. The chemical structures of these compounds are depicted in Figure 1.

A hybrid of 5-nitroindole and 5-nitroimidazole has shown antibacterial activity as a result dual mode of action [60]. However, to the best of my knowledge, the antitrypanosomatid activity of 5-nitroindole-rhodanine conjugates has not been reported yet. Hence, we hypothesized that combining indole, rhodanine, and nitro may provide compounds with enhanced antiprotozoal activity based on the above evidence. Therefore, this study determined the *in vitro* antiparasitic activity, cytotoxicity, and the *in silico* physicochemical and pharmacokinetic properties of a series of 5-nitroindole-rhodanine conjugates. This paper reports and discusses the synthesis of these derivatives and their *in vitro* and *silico* screening outcomes.

2. Experimental

2.1. Materials and methods

The materials and general procedures are reported as Supplementary Material.

2.2. Syntheses

2.2.1. Synthesis of 5-nitro-1 H-indole-3-carbaldehyde (2a)

5-Nitro-1*H*-indole-3-carbaldehyde, **2a** was synthesized by adapting the literature method of Nimbarte et al. [61], and the characterization data are provided as Supplementary Material.

2.2.2. Synthesis of N-alkyl/benzyl 5-nitroindole-3-carbaldehyde derivatives (2b-2f)

A modified protocol of Nimbarte et al. [61] was used to obtain compounds: To a mixture of potassium hydroxide (KOH, 10.5 mmol, 590 mg, 2 equiv.) in dimethylformamide (DMF, 50

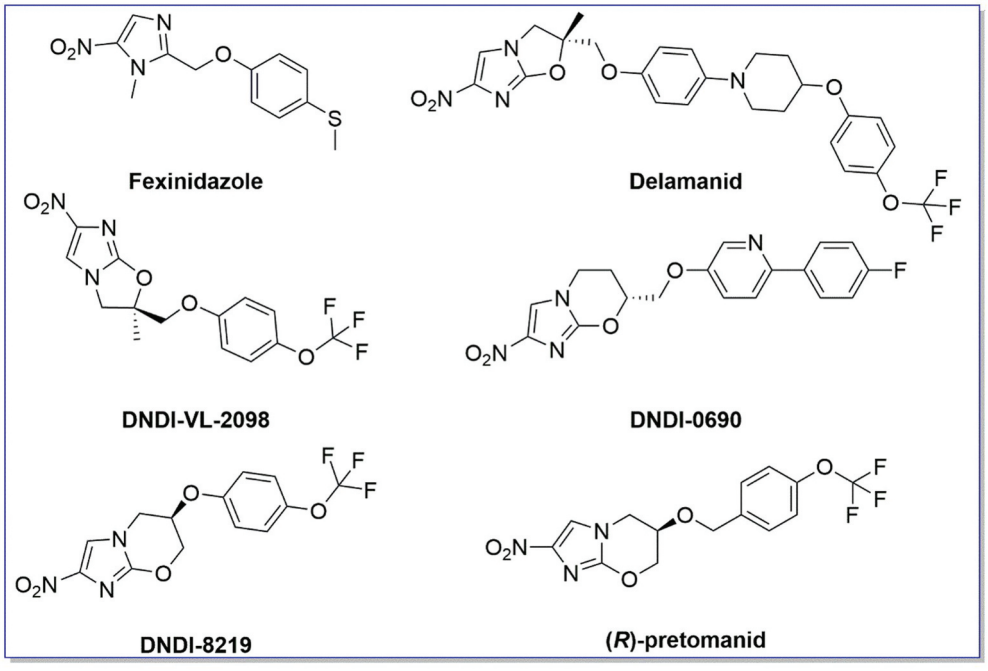

Figure 1. The chemical structures of nitroaromatic compounds with promising in vivo antileishmanial activity.

mL), compound **2a** (5.3 mmol, 1 g, 1 equiv.) was added and allowed to react at room temperature for 30 minutes. Subsequently, the appropriate propargyl/aryl bromide (2–4 equiv.) was added to the reaction mixture and stirred for 12 hours at room temperature until thin-layer chromatography (TLC) monitoring indicated consumption of **2a**. Distilled water of a volume equal to the volume of DMF used in the reaction (50 mL) was then added to the mixture to facilitate precipitation of the crude compound. The precipitate was filtered and washed thoroughly with distilled water. The resultant powder was dried in an oven at 70 °C for two hours. Thereafter, the crude compounds were either purified by dissolving the crude compound in chloroform and precipitating the desired compound out of solution by adding hexane ($CHCl_3$:*n*-Hex 1:2, v/v)(option 1) or recrystallized from DMF (option 2).

2.2.2.1. 5-Nitro-1-(prop-2-yn-1-yl)-1 H-indole-3-carbaldehyde 2b.

2a and propargyl bromide (21.0 mmol, 1.8 mL, 4 equiv.) afforded **2b** as an off-white powder (1 mmol, 221 mg, 92%); mp 202–203.8 °C. IR $_{Vmax}$ (cm^{-1}): 3244 (H-C≡C, stretch), 3130 (H-C=C, stretch), 2831 (H-C=O, stretch), 2130 (C≡C, stretch), 1647 (C=O, stretch), 1585 (C=C, stretch), 1517 (N-O, asymmetric stretch), 1338 (N-O, symmetric stretch). ^{1}H NMR (600 MHz, DMSO-d_6) δ (ppm): 10.03 (s, 1 h, H-8), 8.95 (d, J = 1.9 hz, 1 h, H-4), 8.63 (s, 1 h, H-2), 8.25 (dd, J = 9.0, 1.9 hz, 1 h, H-6), 7.89 (d, J = 9.0 hz, 1 h, H-7), 5.35 (d, J = 2.2 hz, 2 h, H-1′), 3.63 (***t, J = 2.2 hz, 1 h, H-3′). ^{13}C NMR (151 MHz, DMSO-d_6) δ (ppm): 185.3 (C-8), 143.3 (C-7a), 142.8 (C-2), 139.3 (C-5), 124.0 (C-3a), 118.9 (C-4), 118.4 (C-3), 117.2 (C-7), 112.1 (C-6), 77.3 (C-2′), 77.3 (C-3′), 36.5 (C-1′). HRMS-APCI *m/z* $[M+H]^+$: 229.0608 (calc. for $C_{12}H_9N_2O_3^+$, 229.0535). Purity: 98%. ***t coalesced triplet.

2.2.2.2. 1-Benzyl-5-nitro-1 H-indole-3-carbaldehyde 2c.

2a and benzyl bromide (21.0 mmol, 2.5 mL, 4 equiv.) provided **2c** as an off-white powder (2.8 mmol, 780 mg, 53%) after purification by option 1; mp 178.8–179.9 °C. IR $_{Vmax}$ (cm^{-1}): 3093 (H-C=C, stretch), 2807 (H-C=O, stretch), 1657 (C=O, stretch), 1583 (C=C, stretch), 1517 (N-O, asymmetric stretch), 1330 (N-O, symmetric stretch). ^{1}H NMR (600 MHz, $CDCl_3$) δ (ppm): 10.06 (s, 1 h, H-8), 9.22 (*d, J = 1.9 hz, 1 h, H-4), 8.20 (*dd, J = 8.9, 1.9 hz, 1 h, H-6), 7.89 (s, 1 h, H-2), 7.43–7.21 (m, 6 h, H-2,′ H-3,′ H-4,′ H-7), 5.45 (s, 2 h, H-1′). ^{13}C NMR (151 MHz, $CDCl_3$) δ (ppm): 184.0 (C-8), 144.2 (C-7a), 140.4 (C-2), 140.0 (C-5), 134.2 (C-1a′), 129.3 (C-3′), 128.8 (C-4′), 127.2 (C-2′), 124.9 (C-3a), 119.6 (C-3), 119.6 (C-7), 119.0 (C-6), 110.6 (C-4), 51.4 (C-1′). HRMS-APCI *m/z* $[M+H]^+$: 281.0924 (calc. for $C_{16}H_{13}N_2O_3^+$, 281.0848). Purity: 100%. *d coalesced doublet;**dd coalesced doublet of doublets.

2.2.2.3. 1-(4-Methylbenzyl)-5-nitro-1 H-indole-3-carbaldehyde 2d.

2a and 4-methylbenzyl bromide (10.5 mmol, 2 g, 2 equiv.) afforded **2d** as a white powder (3.4 mmol, 992 mg, 64%) after purification by option 1; mp 153.8–155.4 °C. IR $_{Vmax}$ (cm^{-1}): 3108 (H-C=C, stretch), 2819 (H-C=O, stretch), 1655 (C=O, stretch), 1585 (C=C, stretch), 1516 (N-O, asymmetric stretch), 1323 (N-O, symmetric stretch). ^{1}H NMR (600 MHz, $CDCl_3$) δ (ppm): 10.05 (s, 1 h, H-8), 9.22 (d, J = 1.8 hz, 1 h, H-4), 8.20 (dd, J = 9.0, 1.8 hz, 1 h, H-6), 7.87 (s, 1 h, H-2), 7.43 (d, J = 9.0 hz, 1 h, H-7), 7.22 (d, J = 7.8 hz, 2 h, H-2′), 7.12 (d, J = 7.8 hz, 2 h, H-3′), 5.39 (s, 2 h, H-1′), 2.37 (s, 3 h, H-5′). ^{13}C NMR (151 MHz, $CDCl_3$) δ (ppm): 184.0 (C-8), 144.1 (C-7a), 140.4 (C-2), 140.0 (C-5), 138.9 (C-4′), 131.1 (C-1a′), 130.0 (C-3′), 127.4 (C-2′), 125.0 (C-3a), 119.6 (C-7), 119.5 (C-3), 119.0 (C-4), 110.6 (C-6), 51.3 (C-1′), 21.1 (C-5′). HRMS-APCI *m/z* $[M+H]^+$: 295.1093 (calc. for $C_{17}H_{15}N_2O_3^+$, 295.1005). Purity: 100%.

2.2.2.4. 1-(4-Fluorobenzyl)-5-nitro-1 H-indole-3-carbaldehyde 2e.

2a and 4-fluorobenzyl bromide (10.5 mmol, 1.3 mL, 2 equiv.) provided **2e** as a brown powder (2.7 mmol, 789 mg, 50%) after purification by option 1; mp 199.4–202°C. IR $_{Vmax}$ (cm^{-1}): 3108 (H-C=C, stretch), 2824 (H-C=O, stretch), 1649 (C=O, stretch), 1582 (C=C, stretch), 1507 (N-O, asymmetric stretch), 1323 (N-O, symmetric stretch). ^{1}H NMR (600 MHz, $CDCl_3$) δ (ppm): 10.07 (s, 1 h, H-8), 9.22 (d, J = 1.7 hz, 1 h, H-4), 8.20 (dd, J = 9.0, 1.7 hz, 1 h, H-6), 7.87 (s, 1 h, H-2), 7.41 (d, J = 9.0 hz, 1 h, H-7), 7.22 (dd, J = 8.0, 5.2 hz, 2 h, H-2′), 7.11 (t, J = 8.0 hz, 2 h, H-3′), 5.43 (s, 2 h, H-1′). ^{13}C NMR (151 MHz, $CDCl_3$) δ (ppm): 183.9 (C-8), 162.8 (d, J = 249.0 hz, C-4′), 144.2 (C-7a), 140.1 (C-2), 139.8 (C-5), 130.0 (d, J = 3.2 hz, C-1a′), 129.1 (d, J = 8.3 hz, C-2′), 125.0 (C-3a), 119.7 (C-3), 119.7 (C-7), 119.0 (C-6), 116.4 (d, J = 21.9 hz, C-3′), 110.4 (C-4), 50.7 (C-1′). HRMS-APCI *m/z* $[M+H]^+$: 299.0820 (calc. for $C_{16}H_{12}FN_2O_3^+$, 299.0754). Purity: 99%.

2.2.2.5. 1-(3-Chlorobenzyl)-5-nitro-1 H-indole-3-carbaldehyde 2f.

2a and 3-chlorobenzyl bromide (10.5 mmol, 1.4 mL, 2 equiv.) yielded **2f** as a white powder (1.3 mmol, 421 mg, 25%) following purification by option 2; mp 180.5–181.4 °C. IR $_{Vmax}$ (cm^{-1}): 3098 (H-C=C, stretch), 2836 (H-C=O, stretch), 1665 (C=O, stretch), 1579 (C=C, stretch), 1515 (N-O, asymmetric stretch), 1333 (N-O, symmetric stretch). ^{1}H NMR (600 MHz, DMSO-d_6) δ (ppm): 10.04 (s, 1 h, H-8), 8.96 (*d, J = 1.9 hz,1 h, H-4), 8.74 (s, 1 h, H-2), 8.18 (*dd, J = 8.9, 1.9 hz, 1 h, H-6), 7.87 (d, J = 8.9 hz, 1 h, H-7), 7.47 (s, 1 h, H-2′), 7.38 (m, 2 h, H-4,′ H-5′), 7.27 (s, 1 h, H-6′), 5.66 (s, 2 h, H-1′). ^{13}C NMR (151 MHz, DMSO-d_6) δ (ppm): 185.2 (C-8), 143.5 (C-2), 143.2 (C-7a), 139.6 (C-5), 138.5 (C-1a′), 133.3 (C-3′), 130.6 (C-5′), 127.9 (C-2′), 127.2 (C-4′), 126.0 (C-6′), 124.1 (C-3a), 118.8 (C-6), 118.4 (C-3), 117.1 (C-7), 112.0 (C-4), 49.4 (C-1′). HRMS-APCI *m/z* $[M+H]^+$: 315.0535 (calc. for $C_{16}H_{12}ClN_2O_3^+$, 315.0458). Purity: 99%. *d coalesced doublet; **dd coalesced doublet of doublets.

2.2.3. Synthesis of 5-nitroindole-rhodanine conjugates (3a-3f)

The Knoevenagel condensation protocol of Bayindir [62] was slightly modified to obtain the compounds: A mixture of compounds **2a** or **2b-2f** (0.2 g, 1 equiv.), rhodanine (2–6 equiv.), and concentrated ammonia (0.16 mL) in ethanol (EtOH, 6 mL) were heated to boiling. Ammonium chloride (NH_4Cl, 0.5 eq.) dissolved in distilled water (2 mL) was heated to 80 °C and then added dropwise to the reaction mixture. The reaction mixture was then refluxed overnight. Subsequently, the precipitate in the reaction mixture was removed by filtering, washed with distilled water and EtOH, and dried in an oven at 70°C for two hours. DMF was used to recrystallize the crude products when further purification was needed.

2.2.3.1. (Z)-5-[(5-Nitro-1 H-indol-3-yl)methylene]-2-thioxothiazolidin-4-one 3a.

2a and rhodanine (2.1 mmol, 280 mg, 2 equiv.) yielded **3a** as an orange powder (0.9 mmol, 261 mg, 81%); mp 255–255.1 °C. IR $_{Vmax}$ (cm^{-1}): 3253 (N-H, amide, stretch), 3093 (H-C=C, stretch), 1684 (C=O, stretch), 1570 (C=C, stretch), 1518 (N-O, asymmetric stretch), 1307 (N-O, symmetric stretch). ^{1}H NMR (600 MHz, DMSO-d_6) δ (ppm): 13.62 (s, 1 h, H-3''), 12.76 (s, 1 h, H-1), 8.96 (d, J = 1.6 hz, 1 h, H-4), 8.11 (dd, J = 8.9, 1.6 hz, 1 h, H-6), 8.05 (s, 1 h, H-8), 8.00 (s, 1 h, H-2), 7.66 (d, J = 8.9 hz, 1 h, H-7). ^{13}C NMR (151 MHz, DMSO-d_6) δ (ppm): 194.6 (C-2''), 168.9 (C-4''), 142.1 (C-7a), 139.3 (C-5), 132.5 (C-2), 126.1 (C-5''), 123.4 (C-3a), 120.6 (C-8), 118.2 (C-6), 116.0 (C-4), 113.0 (C-7), 112.7 (C-3). HRMS-APCI *m/z* $[M+H]^+$: 306.0013 (calc. for $C_{12}H_8N_3O_3S_2^+$, 305.9929). Purity: 98%.

2.2.3.2. (Z)-5-{[5-Nitro-1-(prop-2-yn-1-yl)-1 H-indol-3-yl] methylene}-2-thioxothiazolidin-4-one 3b.

2b and rhodanine (1.8 mmol, 233 mg, 2 equiv.) supplied **3b** as a yellow powder (0.7 mmol, 244 mg, 81%); mp 288.7–289.7 °C. IR $_{Vmax}$ (cm^{-1}): 3331 (N-H, stretch), 3250 (H-C≡C, stretch), 3064 (H-C=C, stretch), 2123 (C≡C, stretch), 1713 (C=O, stretch), 1599 (C=C, stretch), 1513 (N-O, asymmetric stretch), 1317 (N-O, symmetric stretch). ^{1}H NMR (600 MHz, DMSO-d_6) δ (ppm): 13.66 (s, 1 h, H-3''), 9.03 (*d, J = 1.9 hz, 1 h, H-4), 8.20 (s, 1 h, H-2), 8.10 (*dd, J = 9.0, 1.9 hz, 1 h, H-6), 8.05 (s, 1 h, H-8), 7.83 (*d, J = 9.0 hz, 1 h, H-7), 5.37 (*d, J = 2.2 hz, 2 h, H-1'), 3.57 (***t, J = 2.2 hz, 1 h, H-3'). ^{13}C NMR (151 MHz, DMSO-d_6) δ (ppm): 194.5 (C-2''), 168.9 (C-4''), 142.6 (C-5), 138.5 (C-7a), 134.2 (C-2), 126.8 (C-5''), 122.5 (C-3a), 121.5 (C-8), 118.5 (C-4), 116.4 (C-7), 112.5 (C-3), 111.8 (C-6), 77.6 (C-2'), 77.0 (C-3'), 36.5 (C-1'). HRMS-APCI *m/z* $[M+H]^+$: 344.0170 (calc. for $C_{15}H_{10}N_3O_3S_2^+$, 344.0086). Purity: 99%. *^{d} coalesced doublet; **^{dd} coalesced doublet of doublets; ***^{t} coalesced triplet.

2.2.3.3. (Z)-5-[(1-Benzyl-5-nitro-1 H-indol-3-yl)methylene]-2-thioxothiazolidin-4-one 3c..

2c and rhodanine (1.4 mmol, 190 mg, 2 equiv.) provided **3c** as a yellow powder (0.2 mmol, 86 mg, 31%) after recrystallization from DMF; mp 305.1–306.2°C. IR $_{Vmax}$ (cm^{-1}): 3152 (N-H, stretch), 3065 (H-C=C, stretch), 2988 (CH_2, stretch), 1682 (C=O, stretch), 1589 (C=C, stretch), 1518 (N-O, asymmetric stretch), 1337 (N-O, symmetric stretch). ^{1}H NMR (600 MHz, DMSO-d_6) δ (ppm) 13.66 (s, 1 h, H-3''), 9.01 (*d, J = 1.9 hz, 1 h, H-4), 8.27 (s, 1 h, H-2), 8.11 (**dd, J = 8.8, 1.3 hz, 1 h, H-6), 8.07 (s, 1 h, H-8), 7.78 (d, J = 8.8 hz, 1 h, H-7), 7.37–7.27 (m, 5 h, H-2,' H-3,' H-4'), 5.67 (s, 2 h, H-1'). ^{13}C NMR (151 MHz, DMSO-d_6) δ (ppm): 194.6 (C-2''), 168.9 (C-4''), 142.4 (C-5), 138.8 (C-7a), 136.3 (C-2), 135.1 (C-1a'), 128.7 (C-3'), 127.8 (C-4'), 127.2 (C-2'), 126.8 (C-5''), 122.6 (C-3a), 121.2 (C-8), 118.3 (C-6), 116.3 (C-4), 112.5 (C-3), 111.96 (C-7), 50.1 (C-1'). HRMS-APCI *m/z* $[M+H]^+$: 396.0474 (calc. for $C_{19}H_{14}N_3O_3S_2^+$, 396.0399). Purity: 100%. *^{d} coalesced doublet; **^{dd} coalesced doublet of doublets.

2.2.3.4. (Z)-5-{[1-(4-Methylbenzyl)-5-nitro-1 H-indol-3-yl] methylene}-2-thioxothiazolidin-4-one 3d.

2d and rhodanine (4.1 mmol, 543 mg, 6 equiv.) afforded **3d** as a yellow powder (0.5 mmol, 217 mg, 78%); mp 282.8–284.2 °C. IR $_{Vmax}$ (cm^{-1}): 3333 (N-H, stretch), 3092 (H-C=C, stretch), 2941 (C-H, alkane, stretch), 1710 (C=O, stretch), 1602 (C=C, stretch), 1524 (N-O, asymmetric stretch), 1328 (N-O, symmetric stretch). ^{1}H NMR (600 MHz, DMSO-d_6) δ (ppm): 13.66 (s, 1 h, H-3''), 9.00 (*d, J = 1.9 hz, 1 h, H-4), 8.25 (s, 1 h, H-2), 8.10 (*dd, J = 9.0, 1.9 hz, 1 h, H-6), 8.06 (s, 1 h, H-8), 7.76 (d, J = 9.0 hz, 1 h, H-7), 7.23 (d, J = 7.4 hz, 2 h, H-2'), 7.15 (d, J = 7.4 hz, 2 h, H-3'), 5.61 (s, 2 h, H-1'), 2.24 (s, 3 h, H-5'). ^{13}C NMR (151 MHz, DMSO-d_6) δ (ppm): 195.0 (C-2''), 169.3 (C-4''), 142.9 (C-5), 139.3 (C-7a), 137.6 (C-2), 135.6 (C-4'), 133.8 (C-1a'), 129.7 (C-3'), 127.7 (C-2'), 127.3 (C-5''), 123.2 (C-3a), 121.6 (C-8), 118.8 (C-6), 116.8 (C-4), 112.9 (C-3), 112.4 (C-7), 50.4 (C-1'), 21.0 (C-5'). HRMS-APCI *m/z* $[M+H]^+$: 410.0634 (calc. for $C_{20}H_{16}N_3O_3S_2^+$, 410.0555). Purity: 100%. *^{d} coalesced doublet; **^{dd} coalesced doublet of doublets.

2.2.3.5. (Z)-5-{[1-(4-Fluorobenzyl)-5-nitro-1H -indol-3-yl] methylene}-2-thioxothiazolidin-4-one 3e.

2e and rhodanine (2.0 mmol, 268 mg, 3 equiv.) yielded **3e** as a yellow powder (0.4 mmol, 143 mg, 52%) after recrystallization from DMF; mp 319.4–320.6 °C. IR $_{Vmax}$ (cm^{-1}): 3164 (N-H, stretch), 3087 (H-C=C, stretch), 1682 (C=O, stretch), 1588 (C=C, stretch), 1520 (N-O, asymmetric stretch), 1325 (N-O, symmetric stretch). ^{1}H NMR (600 MHz, DMSO-d_6) δ (ppm): 13.66 (s, 1 h, H-3''), 9.02 (*d, J = 1.9 hz, 1 h, H-4), 8.28 (s, 1 h, H-2), 8.13 (*dd, J = 8.8, 1.9 hz, 1 h, H-6), 8.07 (s, 1 h, H-8), 7.81 (d, J = 8.8 hz, 1 h, H-7), 7.41 (**dd, J = 7.3, 5.8 hz, 2 h, H-2'), 7.18 (t, J = 7.3 hz, 2 h, H-3'), 5.66 (s, 2 h, H-1'). ^{13}C NMR (151 MHz, DMSO-d_6) δ (ppm): 194.6 (C-2''), 168.8 (C-4''), 161.6 (d, J = 244.2 hz, C-4'), 142.5 (C-5), 138.7 (C-7a), 135.0 (C-2), 132.6 (d, J = 2.7 hz, C-1a'), 129.4 (d, J = 8.4 hz, C-2'), 126.8 (C-5''), 122.6 (C-3a), 121.2 (C-8), 118.3 (C-6), 116.3 (C-3). 115.5 (d, J = 21.6 hz, C-3'), 112.5 (C-4), 111.9 (C-7), 49.3 (C-1'). HRMS-APCI *m/z* $[M+H]^+$: 414.0357 (calc. for $C_{19}H_{13}FN_3O_3S_2^+$, 414.0304). Purity: 96%. *^{d} coalesced doublet; *^{dd} coalesced doublet of doublets.

2.2.3.6. (Z)-5-{[1-(3-Chlorobenzyl)-5-nitro-1 H-indol-3-yl] methylene}-2-thioxothiazolidin-4-one 3f.

2f and rhodanine (3.8 mmol, 508 mg, 6 equiv.) provided **3f** as a yellow powder (0.3 mmol, 133 mg, 49%) after recrystallization from DMF; mp 292.5–293.8 °C. IR $_{Vmax}$ (cm^{-1}): 2996 (N-H, stretch), 2832 (CH_2), 1691 (C=O), 1599 (C=C), 1521 (N-O, asymmetric stretch), 1324 (N-O, symmetric stretch). ^{1}H NMR (600 MHz, DMSO-d_6) δ (ppm): 10.04 (s, 1 h, H-2), 8.96 (*d, J = 1.3 hz, 1 h, H-4), 8.75 (s, 1 h, H-8), 8.18 (**dd, J = 9.0, 1.3 hz, 1 h, H-6), 7.88 (d, J = 9.0 hz, 1 h, H-7), 7.47 (s, 1 h, H-2'), 7.39–7.38 (m, 2 h, H-4,' H-5'), 7.27 (s, 1 h, H-6'), 5.66 (s, 2 h, H-1'). ^{13}C NMR (151 MHz, DMSO-d_6) δ (ppm): 185.2 (C-2''), 143.6 (C-2), 143.2 (C-7a), 139.7 (C-5), 138.5 (C-1a'), 133.3 (C-5''), 130.7 (C-5'), 127.9 (C-2'), 127.3 (C-4'), 126.0 (C-6'), 124.1 (C-3a), 118.9 (C-6), 118.4 (C-3), 117.2 (C-7), 112.1 (C-4), 49.4 (C-1'). HRMS-APCI *m/z* $[M+H]^+$: 430.0102 (calc. for $C_{19}H_{13}ClN_3O_3S_2^+$, 430.0009). Purity: 95%. *^{d} coalesced doublet; **^{dd} coalesced doublet of doublets.

2.2.4. Synthesis of 5-nitroindole-rhodanine Schiff bases (4a-4f)

Under inert conditions, compounds **2a-2f** (0.2 g, 1 equiv.) were suspended together with 3-aminorhodanine (1.5–6 equiv.) in

anhydrous methanol (MeOH, 15 mL). Thereafter, triethylamine (TEA, 1.5–6 equiv.) was added dropwise to the reaction mixture. The reaction mixture was then stirred overnight. Subsequently, the precipitate in the reaction mixture was filtered off, washed with distilled water and MeOH, and dried in an oven at 70 °C for two hours to afford the target compounds **4a**, **4b**, and **4e**. However, crudes were further recrystallized from DMF to yield pure **4c**, **4d**, and **4f**.

2.2.4.1. (E)-3-{[(5-Nitro-1 H-indol-3-yl)methylene]amino}-2-thioxothiazolidin-4-one 4a.

2a, 3-aminorhodanine (3.2 mmol, 468 mg, 3 equiv.) and TEA (3.2 mmol, 0.4 mL, 3 equiv.) afforded **4a** as a brown powder (0.6 mmol, 187 mg, 55%); mp 302.8–302.9 °C. IR $_{Vmax}$ (cm^{-1}): 3205 (N-H, stretch), 1702 (C=N, stretch), 1591 (C=C, stretch), 1521 (N-O, asymmetric stretch), 1311 (N-O, symmetric stretch). ^{1}H NMR (600 MHz, DMSO-d_6) δ (ppm): 12.72 (s, 1 h, H-1), 9.02 (d, J = 1.6 hz, 1 h, H-4), 8.27 (s, 1 h, H-2), 8.11 (dd, J = 8.9, 1.6 hz, 1 h, H-6), 8.09 (s, 1 h, H-8), 7.66 (d, J = 8.9 hz, 1 h, H-7), 5.95 (s, 2 h, H-5″). ^{13}C NMR (151 MHz, DMSO-d_6) δ (ppm): 185.9 (C-2″), 163.1 (C-4″), 142.3 (C-7a), 139.3 (C-5), 133.1 (C-2), 126.1 (C-8), 125.4 (C-3a), 118.3 (C-6), 116.1 (C-4), 115.0 (C-5″), 113.0 (C-7), 112.7 (C-3). HRMS-APCI m/z $[M+H]^+$: 321.0104 (calc. for $C_{12}H_9N_4O_3S_2^+$, 321.0038). Purity: 99%.

2.2.4.2. (E)-3-({[5-Nitro-1-(prop-2-yn-1-yl)-1 H-indol-3-yl]methylene}amino)-2-thioxothiazolidin-4-one 4b.

2b, 3-aminorhodanine (1.3 mmol, 195 mg, 1.5 equiv.) and TEA (1.3 mmol, 0.2 mL, 1.5 equiv.) yielded **4b** as a brown powder (0.4 mmol, 138 mg, 44%); mp 206.1–206.2 °C. IR $_{Vmax}$ (cm^{-1}): 3275 (H-C≡C, stretch), 3101 (H-C=C, stretch), 1697 (C=N, stretch), 1596 (C=C, stretch), 1521 (N-O, asymmetric stretch), 1336 (N-O, symmetric stretch). ^{1}H NMR (600 MHz, DMSO-d_6) δ (ppm): 9.10 (d, J = 1.9 hz, 1 h, H-4), 8.27 (s, 1 h, H-2), 8.21 (dd, J = 9.1, 1.9 hz, 1 h, H-6), 8.19 (s, 1 h, H-8), 7.84 (d, J = 9.1 hz, 1 h, H-7), 5.95 (s, 2 h, H-5″), 5.38 (d, J = 2.1 hz, 2 h, H-1′), 3.58 (***t, J = 2.1 hz, 1 h, H-3′). ^{13}C NMR (151 MHz, DMSO-d_6) δ (ppm): 185.9 (C-2″), 163.1 (C-4″), 142.7 (C-7a), 138.4 (C-5), 134.7 (C-2), 126.8 (C-8), 124.4 (C-3a), 118.5 (C-6), 116.5 (C-4), 116.0 (C-5″), 112.5 (C-3), 111.8 (C-7), 77.5 (C-2′), 76.9 (C-3′), 36.5 (C-1′). HRMS-APCI m/z $[M+H]^+$: 359.0287 (calc. for $C_{15}H_{11}N_4O_3S_2^+$, 359.0195). Purity: 91%.

2.2.4.3. (E)-3-{[(1-Benzyl-5-nitro-1 H-indol-3-yl)methylene]amino}-2-thioxothiazolidin-4-one 4c.

2c, 3-aminorhodanine (1.1 mmol, 159 mg, 1.5 equiv.) and TEA (1.1 mmol, 0.2 mL, 1.5 equiv.) provided **4c** as a yellow powder (0.3 mmol, 103 mg, 35%) after recrystallization from DMF; mp 287.7–289.9 °C. IR $_{Vmax}$ (cm^{-1}): 3295 (H-C=C, stretch), 1718 (C=N, stretch), 1703 (C=O, stretch), 1589 (C=C, stretch), 1522 (N-O, asymmetric stretch), 1335 (N-O, symmetric stretch). ^{1}H NMR (600 MHz, DMSO-d_6) δ (ppm): 9.09 (*d, J = 1.9 hz, 1 h, H-4), 8.37 (s, 1 h, H-2), 8.30 (s, 1 h, H-8), 8.13 (**dd, J = 9.0, 1.9 hz, 1 h, H-6), 7.79 (d, J = 9.0 hz, 1 h, H-7), 7.36–7.29 (m, 5 h, H-2,′ H-3,′ H-4′), 5.96 (s, 2 h, H-5″), 5.69 (s, 2 h, H-1′). ^{13}C NMR (151 MHz, DMSO-d_6) δ (ppm): 186.1 (C-2″), 163.2 (C-4″), 142.6 (C-7a), 138.8 (C-5), 136.3 (C-2), 135.6 (C-1a′), 128.7 (C-3′), 127.8 (C-4′), 127.2 (C-2′), 126.9 (C-8), 124.7 (C-3a), 118.4 (C-6), 116.5 (C-4), 115.7 (C-5″), 112.5 (C-3), 112.0 (C-7). HRMS-APCI m/z $[M+H]^+$: 411.0593 (calc. for $C_{19}H_{15}N_4O_3S_2^+$, 411.0508). Purity: 99%. *d coalesced doublet; **dd coalesced doublet of doublets.

2.2.4.4. (E)-3-({[1-(4-Methylbenzyl)-5-nitro-1H -indol-3-yl]methylene}amino)-2-thioxothiazolidin-4-one 4d.

2d, 3-aminorhodanine (2.0 mmol, 302 mg, 3 equiv.) and TEA (2.0 mmol, 0.3 mL, 3 equiv.) afforded **4d** as an orange powder (0.6 mmol, 261 mg, 90%) after recrystallization from DMF; mp 279.2–281.1 °C. IR $_{Vmax}$ (cm^{-1}): 3307 (H-C=C, stretch), 2919 (C-H, alkane, stretch), 1709 (C=N, stretch), 1596 (C=C, stretch), 1522 (N-O, asymmetric stretch), 1328 (N-O, symmetric stretch). ^{1}H NMR (600 MHz, DMSO-d_6) δ (ppm): 9.10 (*d, J = 1.9 hz, 1 h, H-4), 8.37 (s, 1 h, H-2), 8.31 (s, 1 h, H-8), 8.13 (*dd, J = 8.9, 1.9 hz, 1 h, H-6), 7.79 (d, J = 8.9 hz, 1 h, H-7), 7.24 (d, J = 7.3 hz, 2 h, H-2′), 7.15 (d, J = 7.3 hz, 2 h, H-3′), 5.97 (s, 2 h, H-5″), 5.63 (s, 2 h, H-1′), 2.24 (s, 3 h, H-5′). ^{13}C NMR (151 MHz, DMSO-d_6) δ (ppm): 186.5 (C-2″), 163.6 (C-4″), 143.0 (C-5), 139.2 (C-7a), 137.6 (C-2), 136.1 (C-4′), 133.7 (C-1a′), 129.7 (C-3′), 127.7 (C-2′), 127.4 (C-8), 125.2 (C-3a), 118.8 (C-6), 116.9 (C-3), 116.1 (C-5″), 112.9 (C-4), 112.5 (C-7), 50.4 (C-1′), 21.0 (C-5′). HRMS-APCI m/z $[M+H]^+$: 425.0722 (calc. for $C_{20}H_{17}N_4O_3S_2^+$, 425.0664). Purity: 98%. *d coalesced doublet; **dd coalesced doublet of doublets.

2.2.4.5. (E)-3-({[1-(4-Fluorobenzyl)-5-nitro-1 H-indol-3-yl]methylene}amino)-2-thioxothiazolidin-4-one 4e.

3e, 3-aminorhodanine (4.0 mmol, 596 mg, 6 equiv.) and TEA (4.0 mmol, 0.6 mL, 6 equiv.) provided **4e** as an orange powder (0.6 mmol, 268 mg, 93%); mp 303.2–305.1 °C. IR $_{Vmax}$ (cm^{-1}): 3300 (H-C=C, stretch), 1718 (C=N, stretch), 1704 (C=O, stretch), 1598 (C=C, stretch), 1522 (N-O, asymmetric stretch), 1333 (N-O, symmetric stretch). ^{1}H NMR (600 MHz, DMSO-d_6, 80 ºC) δ (ppm): 9.10 (d, J = 2.1 hz, 1 h, H-4), 8.38 (s, 1 h, H-2), 8.32 (s, 1 h, H-8), 8.15 (dd, J = 9.1, 2.1 hz, 1 h, H-6), 7.84 (d, J = 9.1 hz, 1 h, H-7), 7.43 (dd, J = 8.6, 5.5 hz, 2 h, H-2′), 7.19 (t, J = 8.6 hz, 3 h, H-3′), 5.96 (s, 2 h, H-5″), 5.69 (s, 2 h, H-1′). HRMS-APCI m/z $[M+H]^+$: 429.0499 (calc. for $C_{19}H_{14}FN_4O_3S_2^+$, 429.0413). Purity: 93%.

2.2.4.6. (E)-3-({[1-(3-Chlorobenzyl)-5-nitro-1 H-indol-3-yl]methylene}amino)-2-thioxothiazolidin-4-one 4f.

2f, 3-aminorhodanine (3.8 mmol, 565 mg, 6 equiv.), and TEA (3.8 mmol, 0.5 mL, 6 equiv.) yielded **4f** as a yellow powder (0.2 mmol, 94 mg, 33%) after recrystallization from DMF; mp 276.1–277.9 °C. IR $_{Vmax}$ (cm^{-1}): 3310 (H-C=C, stretch), 1725 (C=N, stretch), 1716 (C=O, stretch), 1597 (C=C, stretch), 1523 (N-O, asymmetric stretch), 1329 (N-O, symmetric stretch). ^{1}H NMR (600 MHz, DMSO-d_6) δ (ppm): 9.10 (*d, J = 1.9 hz, 1 h, H-4), 8.40 (s, 1 h, H-2), 8.31 (s, 1 h, H-8), 8.15 (*dd, J = 8.9, 1.9 hz, 1 h, H-6), 7.82 (d, J = 8.9 hz, 1 h, H-7), 7.47 (s, 1 h, H-2′), 7.39–7.36 (m, 2 h, H-4,′ H-5′), 7.27 (s, 1 h, H-6′), 5.96 (s, 2 h, H-5″), 5.70 (s, 2 h, H-1′). ^{13}C NMR (151 MHz, DMSO-d_6) δ (ppm): 186.1 (C-2″), 163.2 (C-4″), 142.6 (C-7a), 138.7 (C-2), 135.6 (C-5), 134.8 (C-3′), 133.3 (C-1a′), 130.6 (C-5′), 127.8 (C-2′), 127.1 (C-4′), 126.9 (C-8), 125.8 (C-6′), 124.6 (C-3a), 118.6 (C-6), 116.5 (C-4), 115.9 (C-5″), 112.6 (C-3), 111.9 (C-7), 49.4 (C-1′). HRMS-APCI m/z $[M+H]^+$: 445.0172 (calc. for $C_{19}H_{14}ClN_4O_3S_2^+$, 445.0118). Purity: 99%. *d coalesced doublet; **dd coalesced doublet of doublets.

2.3. Predicted pharmacokinetic properties

SwissADME (http://www.swissadme.ch), a free web tool, was used to calculate the physicochemical descriptors and predict the pharmacokinetic properties of the 5-nitroindole-rhodanine conjugates based on their molecular structures and the most appropriate *in silico* approaches [63].

2.4. In vitro biological evaluation

2.4.1. Cytotoxicity assays

2.4.1.1. General (mammalian) cytotoxicity. The cell viability of monkey kidney epithelial cells (Vero cell line) after treatment with the experimental compounds was determined by a resazurin-based cytotoxicity assay, as reported previously by Ndlovu et al. [64].

2.4.1.2. Host cell toxicity. The compounds' toxicity was also assessed on human acute monocytic leukemia cells (THP-1 cell line), the host macrophage cell line. The method described by Zuma et al. was applied [65].

2.4.1.3. Animal cytotoxicity. To assess the potential safety of the compounds in livestock concerning the AT-related species screened, the Cell Counting Kit-8 solution (CCK-8) assay was used to assess cytotoxicity in Madin-Darby bovine kidney (MDBK) cells as reported by Sechoaro et al. [66].

2.4.2. Antileishmanial assays

2.4.2.1. Antipromastigote assay. The antipromastigote activity of synthesized derivatives was evaluated for promastigotes of *L. donovani* (strain 9515 (MHOM/IN/95/9515)) and *L. major* (strain NIH S (MHOM/SN/74/Seidman)) using the resazurin assay according to the procedure set out by Ndlovu et al. [64], which was adapted from Siqueira-Neto et al. [67] and Kulshrestha et al. [68].

2.4.2.2. Intramacrophage antileishmanial assay. The antileishmanial activity of synthesized derivatives against intramacrophage parasites was evaluated using the resazurin assay, and the specified *Leishmania* strains were tested using a modified method by Jain et al. [69] and Njanpa et al. [70], as reported by Zuma et al. [71].

2.4.3. Antitrypanosomal assay

The antitrypanosomal activity against various *Trypanosoma* species was determined, as reported by Sechoaro et al. [66].

3. Results and discussion

3.1. Chemistry

A multi-step process was used to synthesize the series of twelve 5-nitroindole-rhodanine conjugate compounds (Figure 2). These conjugates were categorized into two subseries: (i) 5-nitroindole scaffold bound to rhodanine via an alkene bond attached to the methylene carbon of rhodanine (**3a-f**); (ii) 5-nitroindole bound to rhodanine via an imine bond coupled to the amine functional group of rhodanine (**4a-f**). The compounds were further diversified by introducing propargyl or various benzyl substituents onto the amine functional group of 5-nitroindole.

First, a Vilsmeier-Haack formylation of 5-nitroindole **1** was performed according to the literature procedure [61] to afford 5-nitroindole-3-carbaldehyde (**2a**) in an excellent yield (90%). Second, the amine functional group of **2a** was readily deprotonated by the strong base KOH (pKa 15.7). The resulting conjugate base was subjected to a nucleophilic substitution (S_N) with an excess of commercial propargyl bromide or various benzyl bromides to afford the *N*-alkyl/benzyl 5-nitroindole-3-carbaldehydes **2b-f** in poor to excellent yields (25–92%) [61]. Finally, compounds **2a-2f** were anchored to rhodanine via a Knoevenagel condensation to afford conjugates **3a-f** in poor to good yields (31–81%). This reaction was performed in an ethanol-water mixture (EtOH:H_2O, 3:1, v/v). A combination of ammonium hydroxide (NH_4OH, pKa 9.3) and NH_4Cl (pKa 9.3) served as basic catalysts. Alternatively, aldehydes **2a-2f** were linked to 3-aminorhodanine via a base-catalyzed nucleophilic addition to obtain the 5-nitroindole-rhodanine Schiff bases **4a-f** in poor to excellent yields (33–93%). TEA (pKa 10.8) was used as the base, and MeOH was used as the reaction solvent.

The synthesized compounds were characterized using routine analysis techniques such as nuclear magnetic resonance (NMR), infrared spectroscopy (IR), high-resolution mass spectrometry (HRMS), and high-performance liquid chromatography (HPLC). However, due to its poor solubility in deuterated organic solvents, we were unable to obtain a ^{13}C NMR spectrum for hybrid **4e**.

The success of 5-nitroindole formylation was confirmed on the NMR spectra of compound **2a** by the presence of a singlet (s) indicative of the aldehyde proton H-8 at δ 10.02 ppm on the ^1H NMR spectrum. Furthermore, a peak characteristic of the aldehyde carbon C-8 at δ 185.4 ppm was present on the ^{13}C NMR spectrum. Substitution of 5-nitroindole was supported by the disappearance of the singlet representing the nitrogen-bound proton H-1 on the ^1H NMR spectrum of **2a** (δ 12.71 ppm) and of derivatives **2b-2f**. The occurrence of peaks on the NMR spectra of **2b-2f** corresponding to the propargyl and benzyl substituents also supported the substitution of 5-nitroindole. The ^1H NMR spectrum of product **2b** showed the propargylic protons H-1′ and H-3′ as a doublet (d) at δ 5.35 ppm and a coalesced triplet (t) at δ 3.63 ppm, respectively. These findings corresponded to carbon signals on the ^{13}C NMR spectra at δ 36.5 ppm for C-1,′ δ 77.3 ppm for C-2,′ and δ 77.3 ppm for C-3.′ The benzyl substituents were identified by peaks typical of aromatic protons in the ^1H NMR spectrum region of δ 7.47–7.11 ppm and aromatic carbons in the ^{13}C NMR spectrum region δ 162.8–116.4 ppm. The singlet at δ 5.66–5.39 on the ^1H NMR spectra and a peak at δ 51.4–49.4 ppm on the ^{13}C NMR spectra was attributed to the C-1′ carbon bridge and its corresponding protons. Notably, proton-fluorine and carbon-fluorine couplings were observed on the NMR spectra of the fluorobenzyl-substituted compound **2e**. The signals of the aromatic protons H-2′ and H-3′ on the ^1H NMR spectra were found to be split by the nearby fluorine ($^4J_{H\text{-}2'\text{–}F\text{-}4'}$ = 5.2 hz, $^3J_{H\text{-}3'\text{–}F\text{-}4'}$ = 8.0 hz). Furthermore, the coupling of carbon with fluorine was noted for C-1a′ ($^4J_{C\text{-}1a'\text{–}F\text{-}4'}$ = 3.2 hz), C-2′ ($^3J_{C\text{-}2'\text{–}F\text{-}4'}$ = 8.3 hz), C-3′ ($^2J_{C\text{-}3'\text{–}F\text{-}4'}$ = 21.9 hz), and C-4′ ($^1J_{C\text{-}4'\text{–}F\text{-}4'}$ = 249.0 hz) on the ^{13}C NMR spectra, with the coupling constants decreasing with the distance between fluorine and carbon.

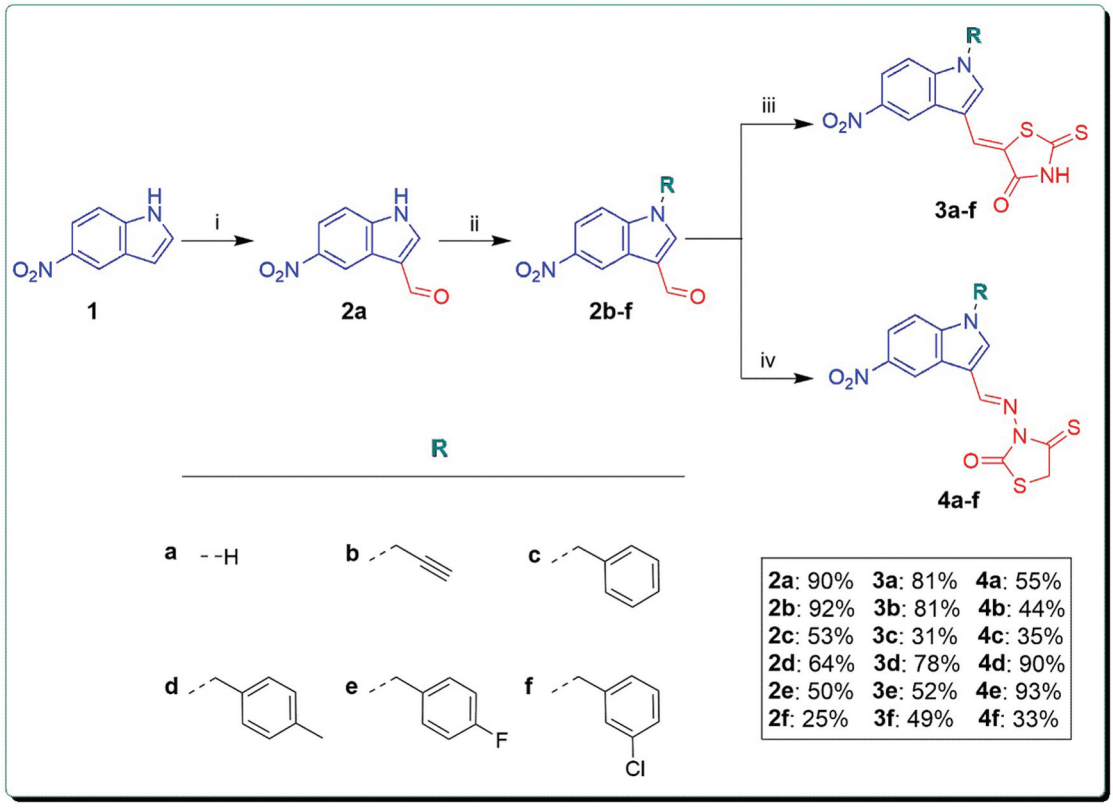

Figure 2. Multi-step synthesis of 5-nitroindole-rhodanine conjugates **3a-4f**.

Reagents and conditions: i. $POCl_3$ (1.5 equiv.), anhydrous DMF, N_2, 0 °C-rt, 2 h; ii. KOH (2 equiv.), DMF, rt, 30 min, propargyl bromide/substituted benzyl bromide (2–4 equiv.), rt, 12 h; iii. Rhodanine (2–6 equiv.), NH_4OH, NH_4Cl (0.5 equiv.), EtOH:H_2O (3:1, v/v), reflux, 12 h; iv. 3-Aminorhodanine (1.5–6 equiv.), TEA (1.5–6 equiv.), anhydrous MeOH, rt, 12 h.

The formation of the Knoevenagel condensation products **3a-f** and the Schiff base condensation products **4a-f** was denoted on the NMR spectra of these compounds by the upfield shift of the peaks indicative of the aldehyde proton and carbon on the NMR spectra of derivatives **2a-f**. Accordingly, the formation of an alkene bond in conjugates **3a-f** was evidenced by a singlet at δ 8.75–8.05 ppm on the ^{1}H NMR spectra attributed to H-8 and a peak at δ 121.6–120.6 ppm on the ^{13}C NMR spectra associated with C-8. The NMR spectra of hybrids **4a-f** revealed a singlet at δ 8.32–8.09 ppm on the ^{1}H NMR spectra accredited to H-8 of the imine bond and a peak at δ 127.4–126.1 ppm on the ^{13}C NMR spectra allocated to C-8 of the imine bond.

The structure of compounds **3a-4f** was further corroborated by peaks that support the presence of the 5-nitroindole and rhodanine moieties. Rhodanine ring is evidenced by: (i) a peak assigned to the thiocarbonyl carbon C-2″ on the ^{13}C NMR spectra in δ 195.0–185.2 ppm; (ii) a peak ascribed to the carbonyl carbon C-4″ on the ^{13}C NMR spectra at δ 169.3–163.1 ppm; (iii) a peak indicative of the carbon C-5″ on the ^{13}C NMR spectra at δ 133.3–126.1 ppm for **3a-f** and δ 116.1–115.0 ppm for **4a-f**; (iv) a singlet at δ 5.97–5.95 ppm on the ^{1}H NMR spectra of **4a-f** suggestive of the methylene proton H-5″; (v) a singlet at δ 13.66–13.62 ppm on the ^{1}H NMR spectra of **3a-f** attributed to the nitrogen-bound proton H-3′.′ The 5-nitroindole scaffold remained intact throughout the multi-step synthesis of the target hybrids. This was evidenced by peaks attributed to the aromatic protons H-2, –3, –4, –6, and –7 on the ^{1}H NMR spectra (δ 10.04–7.21) and aromatic carbons C-2, –3, –3a, –4, –5, –6, –7, and –7a on the ^{13}C NMR spectra (δ 144.2–110.4) of derivatives **2a-4f**. In summary, all protons and carbons of each compound were accounted for.

IR analysis verified the Knoevenagel condensation's success, as demonstrated by the absorption of infrared light by compounds **3a-f** at frequencies associated with H-C=C (3093–3064 cm^{-1}) and C=C bond stretching (1602–1570 cm^{-1}). Absorptions typical of C=N stretching in the 1725–1697 cm^{-1} range supported the formation of Schiff bases **4a-f**. Furthermore, the disappearance of bands at 1665–1647 cm^{-1} and 2836–2807 cm^{-1}, which indicated C=O and H-C=O stretching of the aldehyde functional group in the IR spectra of derivatives **2a-2f**, corroborated the formation of hybrids **3a-4f**. Absorption bands were also witnessed for bonds particular to 5-nitroindole and rhodanine, including N-O asymmetric stretching bands (1529–1507 cm^{-1}), N-O symmetric stretching bands (1338–1307 cm^{-1}), amide N-H stretching bands (3333–2996 cm^{-1}), and amide C=O stretching bands (1716–1682 cm^{-1}). HRMS affirmed the formation of synthesized compounds by detecting each compound's molecular ion on the corresponding mass spectrum. HPLC confirmed the excellent purity of all synthesized compounds (>95%).

3.2. Predicted physicochemical and pharmacokinetic properties

Molecules possessing physicochemical properties comparable to known drugs or advanced clinical candidates are considered drug-like. These favorable physicochemical

properties translate into a good pharmacokinetic and toxicity profile [72]. The pharmacokinetic properties of a molecule, such as its absorption, distribution, metabolism, and elimination (ADME), provide important insights into the access to its therapeutic target. This essential information should be applied in the early stages of drug discovery to filter molecules with ideal ADME properties that can be advanced in the drug development process [63]. Therefore, using the *in-silico* approaches of the web tool SwissADME, the physicochemical descriptors were computed for derivatives **1-4f**. The pharmacokinetic properties, ADME parameters, drug-like nature, and medicinal chemistry friendliness of these compounds were also predicted [63]. The Supplementary Material includes a summary of this data and additional SwissADME prediction data in Tables S1–S3 and Figures S1–S2.

The rule-based filters of Ghose [73], Egan [74], Lipinski [75], Muegge [76], and Veber [77] were applied to test derivatives to predict drug-likeness. All were deemed to be drug-like and presented with favorable physicochemical properties. Similar to the concept of drug-likeness, lead-likeness describes promising lead molecules with physicochemical features that allow for molecular optimization. Lead-like molecules are required to be smaller and less hydrophobic than drug-like ones since leads are subject to chemical modifications that increase their size and lipophilicity [78]. 5-Nitroindole **1** and its derivatives **2a-3a**, **4a**, **and 4b** were found to be lead-like [79].

Since miltefosine is the only oral treatment available for leishmaniasis [15], due consideration was given to predicting the synthesized derivatives' oral absorption and bioavailability. The balance between a drug's solubility in aqueous gastrointestinal (GI) fluids and its permeability through the lipophilic gastrointestinal tract membrane determines the degree of a drug's oral absorption. Lipinski's rule of five is widely used to predict good oral absorption based on the number of hydrogen-bond donors (HBD <5) and hydrogen-bond acceptors (HBA <10), molecular weight (MW < 500), and partition coefficient (logP <5) of the molecule [75]. Accordingly, all the test compounds were predicted to be orally bioavailable. The $logP_{o/w}$, or partition coefficient of a molecule between octanol (lipophilic phase) and water (hydrophilic phase). It characterizes a molecule's lipophilicity and is a valuable indicator of gastrointestinal absorption. Goodwin et al. [80] and Katsuno et al. [81] expanded on Lipinski's rules, limiting the ideal $logP_{o/w}$ for validated hits and leads targeted for infectious disease treatment to 1–3. Thus, only compounds **2b**, **3a**, and **4b** were considered orally bioavailable hits/leads, excluding benzyl-substituted derivatives. The topological polar surface area (TPSA) of a molecule is also valuable in predicting its passive diffusion across biological membranesIt was used in the WLOGP-versus-TPSA referential, or BOILED-Egg model, to predict passive human gastrointestinal absorption (HIA) and blood-brain barrier (BBB) permeation [63,82]. Only test compounds **1-2f** and **3b** were expected to have high gastrointestinal absorption. Moderately polar and relatively lipophilic molecules are more likely to enter the central nervous system (CNS), bridging the BBB. Accordingly, 5-nitroindole **1** and its derivatives **2b-2f** were predicted to penetrate the BBB.

3.3. Pharmacology

3.3.1. Antileishmanial activity

The synthesized compounds, including reaction intermediates, were assessed for *in vitro* antileishmanial activity against *L. major* strain NIH S and antimony-resistant *L. donovani* strain 9515. The selection of *Leishmania* species for this study was motivated by a desire to determine the specificity of the derivatives' antileishmanial efficacy against the causative agents of the disfiguring disease manifestation CL (*L. major*) and the potentially fatal disease manifestation VL (*L. donovani*) [1]. The antileishmanial activity was assessed for both the promastigote stage, found in sand flies, and the intracellular amastigote stage, which infects human macrophages and is clinically relevant. The promastigotes and amastigotes are biochemically distinct and reside in different microenvironments. Therefore, compound activity frequently varies between these parasite stages [67,83]. Intracellular anti-amastigote activity can provide insight into a compound's ability to traverse host macrophage membranes, reach the amastigote in the parasitophorous vacuole, and remain stable in the acidic environment of the vacuole [84]. Such compounds may also exert their effect by targeting host cell factors conducive to parasite survival [85]. Extracellular anti-promastigote activity may reflect antileishmanial activity in the absence of cellular membrane barriers, identifying compounds that may require optimization for permeability and stability to potentially provide anti-amastigote compounds [67].

The cytotoxicity of the compounds was assessed by determining the half-maximal inhibitory concentration (IC_{50}) values against mammalian cell lines at a maximum concentration of 100 µM. The basal cytotoxicity was determined on Vero cells, and emetine (Em) was used as a positive control. Selectivity indices (SI) were calculated to ascertain the selectivity of compounds' toxicity to parasites relative to Vero cells. THP1 cells were used to determine the cytotoxicity of the compounds on the amastigote host cells; AMB was used as a positive control. It is necessary to determine the compounds' toxicity for the host cells of *Leishmania* to identify false positives in the intra-macrophage assay.

Using a maximum concentration of 100 µM to facilitate the determination of structure-activity relationships (SAR), the IC_{50} of each derivative for promastigotes was determined. Then, the percentage growth inhibition of amastigotes was determined for the derivatives at a single concentration of 100 µM. Compounds with > 90% growth inhibition may translate into compounds with a clinically relevant IC_{50} <10 µM and were selected for establishing their IC_{50} values for macrophage-resident amastigotes. AMB, a drug used in the treatment of CL and VL, served as the standard drug. Specificity indexes (SpI) were calculated to ascertain the specificity of activity toward promastigotes or amastigotes.

Furthermore, an activity gain (AG) was calculated when both the precursor **1** and a derivative were active. The cellular potency (IC_{50}) of **1** was divided by that of the derivative to assess whether significant activity differences occurred between them. This can be used to judge further the impact of the chemical transformation and worthiness of the study.

Table 1. The cytotoxicity and antileishmanial activity (μM ± standard deviation) of test compounds against *L. donovani* strain 9515.

			Antipromastigote activity			Static anti-amastigote activity			Cidal anti-amastigote activity		
Compd.	General cytotoxicity Vero IC_{50} (μM)	Host cell cytotoxicity THP-1 IC_{50} (μM)	IC_{50} (μM)	SI_1[a]	AG	IC_{50} (μM)	SI_2[b]	SpI_1[d]	IC_{50} (μM)	SI_3[c]	SpI_2[e]
1	79.51 ± 14.87	>100	50.27 ± 1.36	2	1	>10			>10		
2a	>100	–	>100	–	–	>10	–	–	>10	–	
2b	>100	91.11 ± 12.57	>100	–	–	>10	–	–	>10	–	
2c	>100	>100	>100	–	–	3.61 ± 0.06	28	28	3.57 ± 0.43	28	28
2d	96.91 ± 5.35	>100	0.83 ± 0.02	117	61	>10	–	–	>10	–	–
2e	>100	>100	92.49 ± 10.63	1	0.5	>10	–	–	>10	–	–
2f	99.91 ± 0.13	>100	>100	–	–	>10	–	–	>10	–	–
3a	15.19 ± 0.32	>100	>100	–	–	>10	–	–	>10	–	–
3b	13.51 ± 0.80	–	68.70 ± 6.55	0.2	0.7	>10	–	–	>10	–	–
3c	18.76 ± 3.22	>100	>100	–	–	2.94 ± 0.67	6	34	3.01 ± 0.75	6	33
3d	98.18 ± 1.62	>100	87.40 ± 17.83	1	0.6	5.22 ± 0.65	19	17	5.91 ± 0.60	17	15
3e	17.37 ± 1.33	–	>100	–	–	>10	–	–	>10	–	–
3f	22.24 ± 1.65	>100	19.11 ± 3.70	1	2.6	1.86 ± 0.05	12	10	2.02 ± 0.03	11	10
4a	>100	–	>100	–	–	>10	–	–	>10	–	–
4b	>100	>100	>100	–	–	>10	–	–	>10	–	–
4c	>100	>100	>100	–	–	>10	–	–	>10	–	–
4d	>100	–	>100	–	–	>10	–	–	>10	–	–
4e	>100	–	>100	–	–	>10	–	–	>10	–	–
4f	58.81 ± 13.19	–	>100	–	–	>10	–	–	>10	–	–
Em	0.09 ± 0.009	–	–	–	–	–	–	–	–	–	–
AMB	57.80 ± 3.20	14.86 ± 0.09	0.02 ± 0.009	2890	–	0.05 ± 0.00	1 156	0.40	0.45 ± 0.05	128	0.04

[a]Selectivity Index of *L. donovani*: $SI_1 = IC_{50}$ Vero/IC_{50} promastigote.
[b]Selectivity Index of *L. donovani*: $SI_2 = IC_{50}$ Vero/static IC_{50} amastigote.
[c]Selectivity Index of *L. donovani*: $SI_3 = IC_{50}$ Vero/cidal IC_{50} amastigote.
Specificity index (SpI) < 0.4 indicates more antipromastigote activity, 0.4 < SpI < 2.0 indicates activity against both forms, SpI > 2.0 indicates more anti-amastigote activity [85].
[d]Specificity index of L. donovani: SpI1 = IC50 promastigote/static IC50 amastigote.
[e]Specificity index of L. donovaniy: SpI2 = IC50 promastigote/cidal IC50 amastigote.
Vero: African green monkey kidney epithelial cells; THP-1: human acute monocytic leukemia; Red = compounds qualifying as early antileishmanial leads [81]; Blue = compounds qualifying as antileishmanial hits [81]. AG = Activity gain (IC50 (1)/IC50 (compd.). All data reported in the tables were significant at $p < 0.05$.

Table 2. The antileishmanial activity (μM ± standard deviation) of test compounds against *L. major* strain NIH S.

	Antipromastigote activity			Static anti-amastigote activity			Cidal anti-amastigote activity		
Compd.	IC_{50} (μM	SI_4[f]	AG	IC_{50} (μM)	SI_5[g]	SpI_3[i]	IC_{50} (μM)	SI_6[h]	SpI_4[j]
1	45.80 ± 5.47	2	1	>10	–	–	>10	–	–
2a	>100	–	–	>10	–	–	>10	–	–
2b	>100	–	–	2.43 ± 0.19	41	41	2.41 ± 0.10	41	42
2c	>100	–	–	>10	–	–	>10	–	–
2d	1.42 ± 0.60	68	32.3	>10	–	–	>10	–	–
2e	97.20 ± 3.97	1	0.5	13.12 ± 0.38	8	7	12.89 ± 0.40	8	8
2f	8.75 ± 1.91	11	5.3	9.64 ± 0.45	10	1	13.97 ± 2.79	7	1
3a	>100	–	–	0.60 ± 0.02	25	166	0.57 ± 0.02	27	175
3b	56.78 ± 5.57	0.2	0.9	>10	–	–	>10	–	–
3c	>100	–	–	0.53 ± 0.01	35	189	0.51 ± 0.02	37	196
3d	>100	–	–	1.26 ± 0.14	78	79	0.92 ± 0.13	107	107
3e	>100	–	–	>10	–	–	>10	–	–
3f	17.68 ± 0.90	1	2.6	4.47 ± 0.09	5	4	2.73 ± 0.89	8	7
4a	>100	–	–	>10	–	–	>10	–	–
4b	>100	–	–	9.01	11	11	8.60 ± 1.99	12	12
4c	>100	–	–	2.65 ± 0.16	38	38	2.44 ± 0.33	41	41
4d	70.94 ± 14.29	1	0.7	>10	–	–	>10	–	–
4e	>100	–	–	>10	–	–	>10	–	–
4f	>100	–	–	>10	–	–	>10	–	–
Em	–	–	–	–	–	–	–	–	–
AMB	0.11 ± 0.01	525	–	0.76 ± 0.11	76	0.1	0.75 ± 0.01	77	0.2

[f]Selectivity Index of *L. major*: $SI_4 = IC_{50}$ Vero/IC_{50} promastigote.
[g]Selectivity Index of *L. major*: $SI_5 = IC_{50}$ Vero/static IC_{50} amastigote.
[h]Selectivity Index of *L. major*: $SI_6 = IC_{50}$ Vero/cidal IC_{50} amastigote.
Specificity index (SpI) < 0.4 indicates more antipromastigote activity, 0.4 < SpI < 2.0 indicates activity against both forms, SpI > 2.0indicates more anti-amastigote activity [85].
[i]Specificity index of L. major: SpI3 = IC50 promastigote/static IC50 amastigote.
[j]Specificity index of L. major: SpI4 = IC50 promastigote/cidal IC50 amastigote.
Vero: African green monkey kidney epithelial cells; AG = Activity gain (IC50 (1)/IC50 (compd.; THP-1: human acute monocyticleukaemia; Red = compounds qualifying as early antileishmanial leads and Blue = compounds qualifying as antileishmanial hits [81]. All data reported in the tables were significant at $p < 0.05$.

All the results are reported in Tables 1 and 2 and depicted in Figures 3–5.

Most compounds displayed weak to low toxicity (50 µM<IC_{50} >100 µM) to both Vero and THP-1 cells, which was less than the toxicity of the positive controls [86,87]. However, **3a**, **3b**, **3c**, **3e**, and **3f** were moderately toxic to Vero cells (10 µM<IC_{50} <50 µM) [86,88].

A paucity of derivatives was found to have significant anti-promastigote activity (IC_{50} <10 µM). These derivatives included **2d**, which possessed nanomolar activity against *L. donovani* promastigotes, as well as **2d** and **2f**, which exhibited micromolar activity against *L. major* promastigotes. Contrastingly, a greater number of compounds presented with notable activity (IC_{50} <10 µM) toward amastigotes of both species. For example, **2c**, **3c**, **3d**, and **3f** that showed activity toward *L. donovani* and **2b**, **2f**, **3a**, **3c**, **3d**, **3f**, **4b**, and **4c** that showed activity toward *L. major*. As such, the specificity indices of the derivatives were significant (SpI 4–189). Benzylated indole **2f** was singular because it presented substantial activity against both promastigotes and amastigotes of *L. major* (SpI 0.9). The 5-nitroindole-rhodanine conjugates may thus possess some of the ideal features previously stated as required for anti-amastigote activity. Notably, compared to *L. donovani*, more compounds showed significant activity against *L. major*. 5-Ene-rhodanine derivatives **3c**, **3d**, and **3f** had considerable activity toward amastigotes of both *L. major* and *L. donovani* strains.

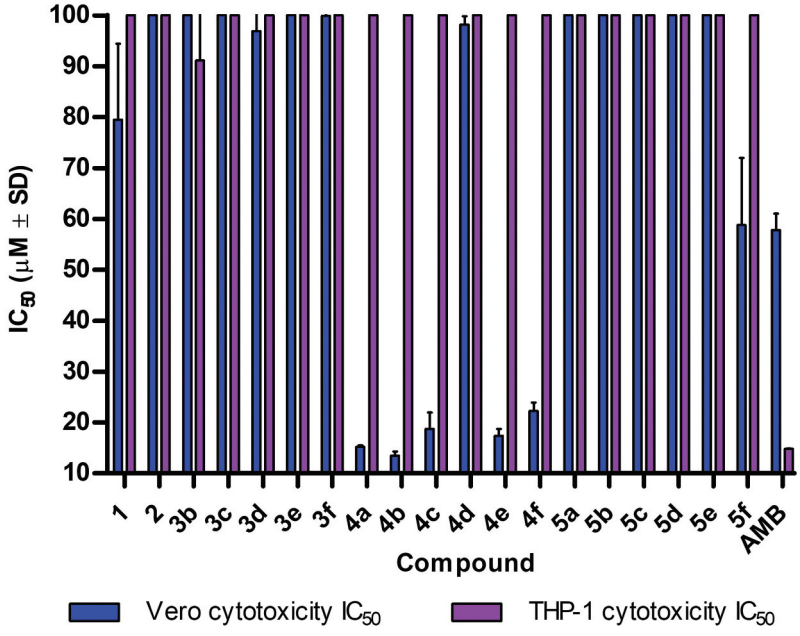

Figure 3. The variation of the cytotoxicity (µM ± standard deviation) of compounds **1–4f** against mammalian cell lines.

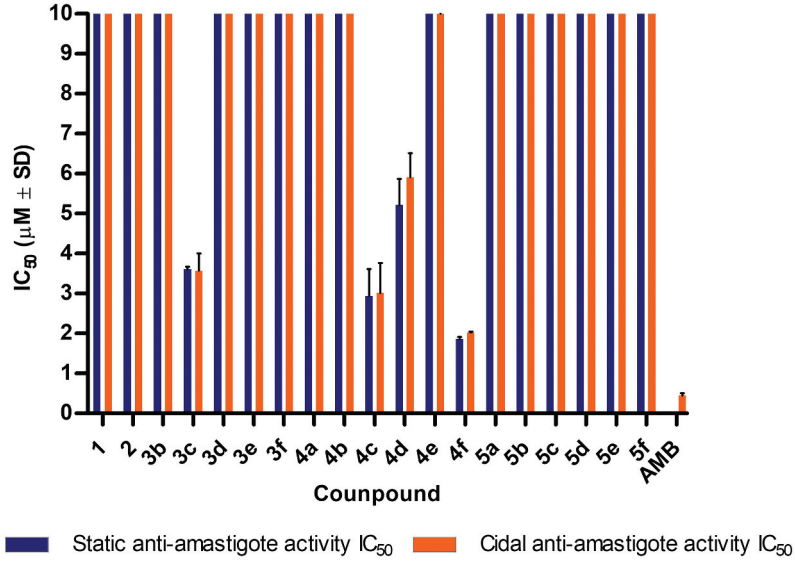

Figure 4. The variation of the antileishmanial activity (µM ± standard deviation) of compounds **1–4f** against L. donovani strain 9515.

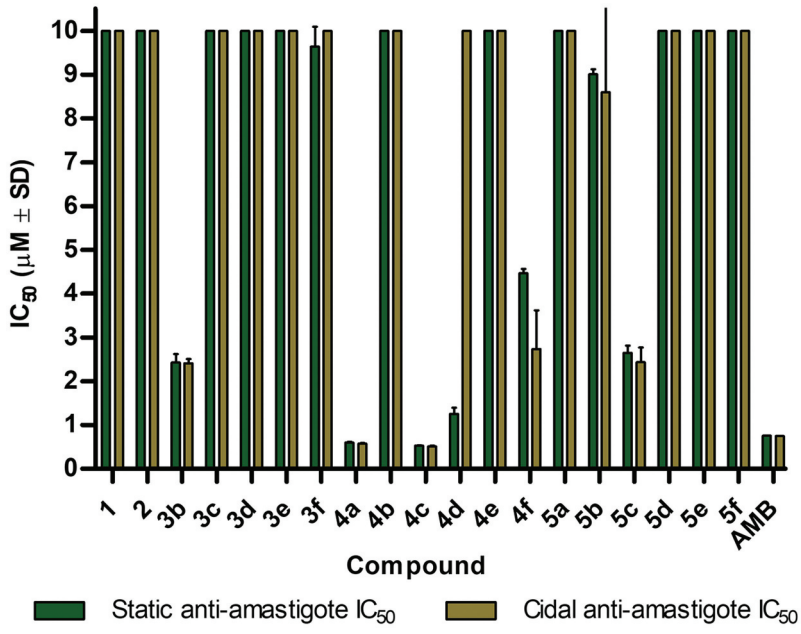

Figure 5. The variation of the antileishmanial activity (μM ± standard deviation) of compounds **1-4f** against L. major strain NIH S.

Most tested compounds' antipromastigote and anti-amastigote activity were inferior to the activity of the standard drug AMB.

To identify promising antileishmanial compounds, the hit/lead criteria for treating infectious diseases of developing countries compiled by the Japanese Global Health Innovative Technology (GHIT) Fund and partners and reported by Katsuno et al. [81] were applied to the screening results. According to these criteria, a hit for VL should present with an IC_{50} <10 μM for intracellular *L. donovani* and selective toxicity toward parasites over mammalian cells, as represented by an SI > 10. Similarly, a lead for VL should be presented with an IC_{50} <1 μM for intracellular *L. donovani* in conjunction with an SI > 100.

Derivatives **2c**, **3d**, and **3f** were identified as hits with micromolar activity toward *L. donovani* amastigotes. Despite its potent activity against *L. donovani* amastigotes, conjugate **3c** (IC_{50} 3.01 ± 0.75 μM), was excluded as a hit due to its moderate cytotoxicity on Vero cells, which resulted in an SI < 10. Compounds **2b**, **3a**, **3c**, **4b**, and **4c** qualified as hits against *L. major* amastigotes. The 5-nitroindole-rhodanine conjugate **3a** (IC_{50} 0.57 ± 0.02 μM) and **3c** (IC_{50} 0.51 ± 0.02 μM) were the most potent and exhibited nanomolar activity comparable to AMB (IC_{50} 0.75 ± 0.01 μM). However, these compounds were shown to have moderate toxicity on Vero cells. Therefore, their selectivity indices were not as considerable as that of AMB (SI **3a** 27, **3c** 37 vs. AMB 77). Hybrid **3f** exhibited potent activity against *L. major* (IC_{50} 2.73 ± 0.89 μM). Still, it was disqualified as a hit due to its moderate cytotoxicity on Vero cells, which resulted in an SI of 8.

Moreover, indole derivative **2d** had early lead-like antipromastigote activity against *L. donovani* (IC_{50} 0.83 ± 0.02 μM; SI 117), with no activity against promastigotes of *L. major* and amastigotes of both strains. Although promastigotes are not clinically relevant, **2d** was predicted to be lead-like, and its ease of optimization may enhance its anti-amastigote activity. This was confirmed by the potent anti-amastigote activity displayed by its -ylidene congener, **3d**, against both *L. donovani* and *L. major*. Yet its Schiff base counterpart, **4d**, was inactive. 5-Ene-rhodanine derivative **3d** also presented submicromolar activity against the amastigotes of *L. major* (IC_{50} 0.92 ± 0.13 μM) and a low toxicity on Vero cells, with a high SI of 107. Accordingly, it was considered a potential early lead for *L. major* and a hit for *L. donovani*. Although the anti-amastigote activity of this conjugate toward *L. major* was inferior to the reference drug AMB, it presented with a significantly better cytotoxicity profile than AMB. Despite the predicted low gastrointestinal absorption by the WLOGP-versus-TPSA referential, **3d** was considered drug-like and orally bioavailable by Lipinski and other rule-based filters, hence merits further attention.

Anti-amastigote active compounds may exert their effects by inhibiting parasite proliferation (static activity) or causing parasite death (cidal activity). Following treatment by a compound with static activity, surviving amastigotes can recover, convert back into promastigotes, and resume proliferation. The IC_{50} determined 24 hours after lysis does not indicate the nature of the anti-amastigote activity. Therefore, the amastigotes could recover from a static treatment through incubation for up to 72 hours following lysis. A substantial decline in a compound's IC_{50} between 24- and 72 hours post-lysis indicates static activity. Accordingly, most derivatives were determined to be cidal in nature, as evidenced by the preserved anti-amastigote activity between 24- and 72 hours after lysis. Exceptionally, aldehyde **2f** displayed static anti-amastigote activity toward *L. major*, which, while considerable (IC_{50} 9.64 ± 0.45 μM), resulted in its rejection as a hit compound.

Furthermore, no AG was deduced as the precursor 5-nitroindole **1** was inactive against the clinically relevant

Table 3. Test compounds' antitrypanosomal activity (μM ± standard deviation) against five *Trypanosoma* spp.

Compd.	Cytotoxicity IC_{50} ± SD (μM)[a] MDBK	Antitrypomastigote activity IC_{50} ± SD (μM)[a] (SI)[b] Tbg IL1922	Tbr IL1501	Tbb GuTat3.1	Tc IL3000	Teq IVM-t1
1	x	>154	>154	>154	>154	>154
2a	>526	>131	>131	>131	>131	>131
2b	>438	>110	>110	>110	>110	>110
2c	>357	>89	>89	>89	>89	>89
2d	x	>85	>85	>85	>85	>85
2e	>335	22.40 ± 5.03 (15)	83.82 ± 2.62 (4)	14.95 ± 8.48 (22)	>84	>84
2f	x	>79	>79	>79	>79	>79
3a	31.57 ± 1.67	34.13 ± 0.29 (1)	81.88 ± 2.29 (0)	33.67 ± 5.01 (1)	46.90 ± 7.76 (1)	38.16 ± 0.85 (1)
3b	>312	>78	78.04 ± 2.90 (4)	>78	>78	>78
3c	99.13 ± 0.96	>73	>73	>73	21.32 ± 1.49 (5)	>73
3d	x	>70	>70	>70	>70	>70
3e	16.98 ± 2.65	>63	>63	>63	2.52 ± 0.73 (7)	>63
3f	x	>61	>61	>61	>61	>61
4a	66.84 ± 9.55	>61	>61	>61	>61	>61
4b	x	>59	>59	>59	>59	>59
4c	x	>60	>60	>60	>60	>60
4d	x	>58	>58	>58	>58	>58
4e	22.39 ± 5.37	52.20 ± 5.09 (0)	58.15 ± 3.84 (0)	55.32 ± 4.84 (0)	>58	>58
4f	x	>56	>56	>56	>56	>56
Suramin	>70	0.467 ± 0.08 (150)	0.150 ± 0.04 (467)	0.07 ± 0.02 (1000)	8.46 ± 0.12 (8)	0.071 ± 0.01 (1401)
Diminazine aceturate	>355	0.011 ± 0.00 (33333)	0.039 ± 0.00 (9091)	0.068 ± 0.00 (5263)	0.09 ± 0.00 (4000)	0.022 ± 0.002 (16340)

[a]Half maximal inhibitory concentration (IC_{50}, μM) represented as the mean ± standard deviation (SD), three biological replicates.
[b]Selectivity index (SI): IC_{50} of MDBK/IC_{50} of trypanosome.
MDBK: Madin-Darby bovine kidney cells; *Tbg* IL1922: *T. brucei gambiense* strain IL1922; *Tbr* IL1501: *T. brucei rhodesiense* strain; *Tbb* GUTat3.1: *T. brucei brucei* strain GUTat3.1; *Tc* IL3000: *T. congolense* strain IL3000; *Teq* IVM-t1: *T. equiperdum* strain IVM-t1; X: not screened.

amastigotes of both *L. donovani* and *L. major* strains. However, derivative **2d** showed 68- and 34-fold activity enhancement relative to **1** against the promastigotes of *L. donovani* and *L. major*, respectively. Overall, the chemical transformation and the study are deemed beneficial as they uncovered promising antileishmanial candidates for further *in vivo* study.

3.3.2. Structure-activity relationships

The lack of antileishmanial activity in most derivatives impeded the determination of realistic SAR. Regarding associations with inactivity, poor solubility occurred for several hybrids (**3e-3f** and **4a-4f**) in 100% dimethyl sulfoxide (DMSO) used for sample preparation and in the aqueous screening medium (**3a-3b** and **4b, 4d, 4e**). This may have led to erroneous compound screening concentrations whichmay have contributed to the observed lack of activity for some of these derivatives.

Nevertheless, it was shown that the 5-ene-rhodanine derivatives, apart from **3d**, presented greater toxicity to Vero cells than the Schiff bases. As stated, these conjugates were categorized into two subseries based on binding 5-nitroindole to rhodanine via an alkene bond attached to the methylene carbon (**3a-f**) or an imine bond coupled to the amine functional group of rhodanine (**4a-f**). Notably, the 5-ene bond is potentially reactive. The toxicity of this moiety may have contributed to the leishmanicidal activity of some compounds, for example, **3c** and **3f** against *L. donovani* and *L. major* amastigotes, respectively. The low SI's (<10) of these compounds suggest that their leishmanicidal activity against *L. donovani* or *L. major* amastigotes may be driven by the inherent toxicity of the 5-ene-rhodanine moiety rather than intrinsic antiparasitic effects.

3.3.3. Antitrypanosomal activity

The compounds were also assessed for *in vitro* antitrypanosomal activity against HAT subspecies *T. b. gambiense* strain IL1922 and *T. b. rhodesiense* strain IL1501, as well as AT subspecies *T. b. brucei* strain GUTat3.1, *T. congolense* strain IL3000, *T. equiperdum* strain IVM-t1. Antitrypanosomal drugs suramin and diminazene aceturate served as reference drugs. The cytotoxicity of the compounds in animals was assessed by determining the IC_{50} values against MDBK cells. The results are summarized in Table 3.

Analogue **3c** presented with the highest activity (IC_{50} 2.5 μM) against *T. congolense*, but the activity was deemed not intrinsic due to a similar level of MDBK cytotoxicity as observed in Vero cells. Compounds **2e** and **3b** showed some activity (IC_{50} 20–40 μM) against several *Trypanosoma* spp., though the activity was not deemed significant if Katsuno *et al*. [81]'s guidelines are taken into consideration. As with the antileishmanial activity, no sufficient antitrypanosomal activities were available for clear SAR determination.

4. Conclusion

A series of 5-nitroindole-rhodanine conjugates were synthesized in poor to excellent yields. Most of these compounds were found to have low toxicity toward mammalian cell lines. However, the 5-ene-rhodanine conjugates presented with moderate toxicity to Vero cells. Nine hits were uncovered with leishmanicidal activity toward *L. major* and/or *L. donovani*. These compounds appeared to target *L. major* over *L. donovani*. Furthermore, the compounds presented with limited activities against the five tested *Trypanosoma* spp., which may indicate selectivity toward *Leishmania* spp. To the hits' advantage, all were predicted to be drug-like and orally

bioavailable by Lipinski's rule of five. 3-Chlorobenzyl-substituted conjugate **3f** was the most promising hit against the lethal *L. donovani* species. 4-Methylbenzyl-substituted conjugate **3d** was identified as a potential early lead compound toward the stigmatizing *L. major* species. Therefore, these derivatives deserve further attention in future studies. It would be interesting for future investigations to uncover these hits' mechanisms of action, determine whether the activity is due to the metabolically active nitro group or the reactivity of rhodanine, and identify their possible biological target/s. The remaining 5-nitroindole-rhodanine conjugates may benefit from structural modifications that increase their solubility in the screening medium and, possibly, their activity.

Funding

This work was based upon research financially supported by the National Research Foundation (NRF) under grant [UID 140476], the Japan Society for the Promotion of Science (JSPS) under [Grant Number 148781], and the North-West University, Potchefstroom Campus. The authors thank Dr. Johan H.L. Jordaan for the HRMS analysis and Dr. Daniel P. Otto for the NMR analysis.

Declaration of Interest

The authors have no relevant affiliations or financial involvement with any organization or entity with a financial interest in or financial conflict with the subject matter or materials discussed in the manuscript. This includes employment, consultancies, honoraria, stock ownership or options, expert testimony, grants or patents received or pending, or royalties.

Disclaimer

Any opinions, findings, conclusions, or recommendations expressed in this material are those of the authors, and therefore, the NRF does not accept any liability in regard thereto.

Data availability statement

The data supporting the findings of this study are provided in the manuscript and the Supplementary information files.

Ethics approval

The current study does not involve human samples. All *in vitro* procedures conducted were approved by the Human Research Ethics Committee of the North-West University (NWU-00223-21-A1), South Africa, and the Obihiro University of Agriculture and Veterinary Medicine, Japan.

Acknowledgments

The following reagents were obtained through BEI Resources, NIAID, NIH: *Leishmania donovani*, Strain 9515 (MHOM/IN/95/9515), NR-48822 *Leishmania major*, Strain NIH S (MHOM/SN/74/Seidman), NR-48819

ORCID

Emce Badenhorst http://orcid.org/0000-0002-5823-2643
Janine Aucamp http://orcid.org/0000-0002-3685-5532
Christina Kannigadu http://orcid.org/0000-0001-9486-8406
Helena D. Janse van Rensburg http://orcid.org/0000-0002-4066-7489
Keisuke Suganuma http://orcid.org/0000-0001-5809-8811
David D. N'Da http://orcid.org/0000-0002-2327-0551

References

Papers of special note have been highlighted as either of interest (•) or of considerable interest (••) to readers.

1. WHO. Leishmaniasis. 2024 [cited 2024 Nov 25]. Available from: https://www.who.int/data/gho/data/themes/topics/gho-ntd-leishmaniasis
2. Leishmaniasis. Level 3 cause. 2024 [cited 2024 Sep]. Available from: https://www.healthdata.org/research-analysis/diseases-injuries-risks/factsheets/2021-leishmaniasis-level-3-disease
3. WHO. Global leishmaniasis surveillance updates 2023: 3 years of the NTD road map. 2024 [cited 2024 Nov 25]. Available from: https://www.who.int/publications/i/item/who-wer-9945-653-669
4. Volpedo G, Pacheco-Fernandez T, Holcomb EA, et al. Mechanisms of immunopathogenesis in cutaneous leishmaniasis and post kala-azar dermal leishmaniasis (PKDL). Front Cell Infect Microbiol. 2021;11:685296. doi: 10.3389/fcimb.2021.685296
5. Costa CHN, Chang KP, Costa DL, et al. From infection to death: an overview of the pathogenesis of visceral leishmaniasis. Pathogens. 2023;12(7):969. doi: 10.3390/pathogens12070969
6. Gurel MS, Tekin B, Uzun S. Cutaneous leishmaniasis: a great imitator. Clin Dermatol. 2020;38(2):140–151. doi: 10.1016/j.clindermatol.2019.10.008
7. Abadias-Granado I, Diago A, Cerro PA, et al. Cutaneous and Mucocutaneous Leishmaniasis. Actas Dermosifiliogr (Engl Ed). 2021;112(7):601–618. doi: 10.1016/j.adengl.2021.05.011
8. Bansal N, Jain A. Diagnosing visceral leishmaniasis. BMJ. 2023;383:e076715. doi: 10.1136/bmj-2023-076715
9. Pires M, Wright B, Kaye PM, et al. The impact of leishmaniasis on mental health and psychosocial well-being: a systematic review. PLOS ONE. 2019;14(10):e0223313. doi: 10.1371/journal.pone.0223313
10. Sunyoto T, Boelaert M, Meheus F. Understanding the economic impact of leishmaniasis on households in endemic countries: a systematic review. Expert Rev Anti Infect Ther. 2019;17(1):57–69. doi: 10.1080/14787210.2019.1555471
11. Engels D, Zhou XN. Neglected tropical diseases: an effective global response to local poverty-related disease priorities. Infect Dis Poverty. 2020;9(1):10. doi: 10.1186/s40249-020-0630-9
12. Alvar J, den Boer M, Dagne DA. Towards the elimination of visceral leishmaniasis as a public health problem in east Africa: reflections on an enhanced control strategy and a call for action. Lancet Glob Health. 2021;9(12):e1763–e1769. doi: 10.1016/S2214-109X(21)00392-2
13. Sharifi I, Khosravi A, Aflatoonian MR, et al. Cutaneous leishmaniasis situation analysis in the islamic Republic of Iran in preparation for an elimination plan. Front Public Health. 2023;11:1091709. doi: 10.3389/fpubh.2023.1091709
14. Control of the leishmaniases: WHO TRS N°949 - report of a meeting of the WHO expert committee on the control of leishmaniases. Geneva; 2010 Mar 22–26 [cited 2025 Feb]. Available from: https://www.who.int/publications/i/item/WHO-TRS-949
15. Roatt BM, de Oliveira Cardoso JM, De Brito RCF, et al. Recent advances and new strategies on leishmaniasis treatment. Appl Microbiol Biotechnol. 2020;104(21):8965–8977. doi: 10.1007/s00253-020-10856-w
16. Wijnant GJ, Dumetz F, Dirkx L, et al. Tackling drug resistance and other causes of treatment failure in leishmaniasis. Front Trop Dis. 2022;3:837460. doi: 10.3389/fitd.2022.837460
17. Field MC, Horn D, Fairlamb AH, et al. Anti-trypanosomatid drug discovery: an ongoing challenge and a continuing need. Nat Rev Microbiol. 2017;15(4):217–231. doi: 10.1038/nrmicro.2016.193
18. Sundar S, Singh B. Emerging therapeutic targets for treatment of leishmaniasis. Expert Opin Ther Targets. 2018 Jun;22(6):467–486. doi: 10.1038/nrmicro.2016.193
19. Franco JR, Cecchi G, Paone M, et al. The elimination of human African trypanosomiasis: achievements in relation to WHO road

map targets for 2020. PLOS Negl Trop Dis. 2022;16(1):e0010047. doi: 10.1371/journal.pntd.0010047
20. Rascón-García K, Martínez-López B, Cecchi G, et al. Prevalence of African animal trypanosomiasis among livestock and domestic animals in Uganda: a systematic review and meta-regression analysis from 1980 to 2022. Sci Rep. 2023;13(1):20337. doi: 10.1038/s41598-023-47141-5
21. Rahman MT, Sobur MA, Islam MS, et al. Zoonotic diseases: etiology, impact, and control. Microorganisms. 2020;8(9):1405. doi: 10.3390/microorganisms8091405
22. Skoreński M, Sieńczyk M. The fellowship of privileged scaffolds—one structure to inhibit them all. Pharmaceuticals. 2021;14(11):1164. doi: 10.3390/ph14111164
23. Senger MR, Fraga CA, Dantas RF, et al. Filtering promiscuous compounds in early drug discovery: is it a good idea? Drug Discov Today. 2016;21(6):868–872. doi: 10.1016/j.drudis.2016.02.004
24. Sravanthi TV, Manju SL. Indoles — a promising scaffold for drug development. Eur J Pharm Sci. 2016;91:1–10. doi: 10.1016/j.ejps.2016.05.025
25. Norwood V, Huigens RW 3rd. Harnessing the chemistry of the indole heterocycle to drive discoveries in biology and medicine. Chembiochem. 2019;20(18):2273–2297. doi: 10.1002/cbic.201800768
26. Bartoli G, Dalpozzo R, Nardi M. Applications of Bartoli indole synthesis. Chem Soc Rev. 2014;43(13):4728–4750. doi: 10.1039/c4cs00045e
27. Taylor SD, Palmer M. The action mechanism of daptomycin. Bioorg Med Chem. 2016;24(24):6253–6268. doi: 10.1016/j.bmc.2016.05.052
28. Greig SL. Osimertinib: first global approval. Drugs. 2016;76(2):263–273. doi: 10.1007/s40265-015-0533-4
29. Lucas S. The pharmacology of indomethacin. Headache. 2016;56(2):436–446. doi: 10.1111/head.12769
30. Zhu W, Bao X, Ren H, et al. N-Phenyl indole derivatives as AT1 antagonists with anti-hypertension activities: design, synthesis and biological evaluation. Eur J Med Chem. 2016;115:161–178. doi: 10.1016/j.ejmech.2016.03.021
31. Kumar RR, Kumar V, Kaur D, et al. Investigation of indole-3-piperazinyl derivatives as potential antidepressants: design, synthesis, in-vitro, in-vivo and in-silico analysis. ChemistrySelect. 2021;6(41):11276–11284. doi: 10.1002/slct.202103568
32. Taha M, Imran S, Salahuddin M, et al. Evaluation and docking of indole sulfonamide as a potent inhibitor of α-glucosidase enzyme in streptozotocin-induced diabetic albino wistar rats. Bioorg Chem. 2021;110:104808. doi: 10.1016/j.bioorg.2021.10480
33. Taha M, Uddin I, Gollapalli M, et al. Synthesis, anti-leishmanial and molecular docking study of bis-indole derivatives. BMC Chem. 2019;13(1):102. doi: 10.1186/s13065-019-0617-4
34. Anand D, Yadav PK, Patel OPS, et al. Antileishmanial activity of pyrazolopyridine derivatives and their potential as an adjunct therapy with miltefosine. J Med Chem. 2017;60(3):1041–1059. doi: 10.1021/acs.jmedchem.6b01447
35. Porwal S, Gupta S, Chauhan PMS. Gem-dithioacetylated indole derivatives as novel antileishmanial agents. Bioorg Med Chem Lett. 2017;27(20):4643–4646. doi: 10.1016/j.bmcl.2017.09.018
•• **This reference holds significant relevance in this study. The authors have drawn upon the results from this reference to establish the rationale for the choice of indole moiety as potential antileishmanial scaffold.**
36. da Silva PR, de Oliveira JF, da Silva AL, et al. Novel indol-3-yl-thiosemicarbazone derivatives: Obtaining, evaluation of in vitro leishmanicidal activity and ultrastructural studies. Chem Biol Interact. 2020;315:108899. doi: 10.1016/j.cbi.2019.108899
37. Schadich E, Kryshchyshyn-Dylevych A, Holota S, et al. Assessing different thiazolidine and thiazole based compounds as antileishmanial scaffolds. Bioorg Med Chem Lett. 2020;30(23):127616. doi: 10.1016/j.bmcl.2020.127616
38. Ihnatenko I, Müller MJ, Orban OCF, et al. The indole motif is essential for the antitrypanosomal activity of N5-substituted paullones. PLOS ONE. 2023;18(11):e0292946. doi: 10.1371/journal.pone.0292946
•• **This reference holds significant relevance in this study. The authors have drawn upon the results from this reference to establish the rationale for the choice of 5-nitroindole moiety as potential antitrypanosomal pharmacophore.**
39. Farahat AA, Ismail MA, Kumar A, et al. Indole and Benzimidazole Bichalcophenes: synthesis, DNA binding and antiparasitic activity. Eur J Med Chem. 2018;143:1590–1596. doi: 10.1016/j.ejmech.2017.10.056
40. Guillon J, Boudot C, Cohen A, et al. Synthesis of 1H–3-{4-[(3-Dimethylaminopropyl)aminomethyl]phenyl}-2-phenylindole and evaluation of its antiprotozoal activity. Molbank. 2019;2019(2):M1060. doi: 10.3390/M1060
41. Kaminskyy D, Kryshchyshyn A, Lesyk R. Recent developments with rhodanine as a scaffold for drug discovery. Expert Opin Drug Discov. 2017;12(12):1233–1252. doi: 10.1080/17460441.2017.1388370
•• **This reference holds significant relevance in this study. The authors have drawn upon the results from this reference to establish the rationale for the choice of rhodanine as a privileged scaffold in drug discovery.**
42. Mendgen T, Steuer C, Klein CD. Privileged scaffolds or promiscuous binders: a comparative study on rhodanines and related heterocycles in medicinal chemistry. J Med Chem. 2012;55(2):743–753. doi: 10.1021/jm201243p
43. Kaminskyy D, Kryshchyshyn A, Lesyk R. 5-ene-4-thiazolidinones - an efficient tool in medicinal chemistry. Eur J Med Chem. 2017;140:542–594. doi: 10.1016/j.ejmech.2017.09.031
•• **This reference holds significant relevance in this study. The authors have drawn upon the results from this reference to establish the rationale for the design and synthesis of 5-ene-rhodanine compounds (3a-3f) with potential antiparasitic pharmacological values.**
44. Wu Y, Ding X, Xu S, et al. Design and synthesis of biaryloxazolidinone derivatives containing a rhodanine or thiohydantoin moiety as novel antibacterial agents against gram-positive bacteria. Bioorg Med Chem Lett. 2019;29(3):496–502. doi: 10.1016/j.bmcl.2018.12.012
45. Havrylyuk D, Zimenkovsky B, Karpenko O, et al. Synthesis of pyrazoline-thiazolidinone hybrids with trypanocidal activity. Eur J Med Chem. 2014;85:245–254. doi: 10.1016/j.ejmech.2014.07.103
46. Jadav SS, Sinha BN, Hilgenfeld R, et al. Thiazolidone derivatives as inhibitors of chikungunya virus. Eur J Med Chem. 2015;89:172–178. doi: 10.1016/j.ejmech.2014.10.042
47. Al Neyadi SS, Adem A, Amir N, et al. Novel thiazolidinedione and rhodanine derivatives regulate glucose metabolism, improve insulin sensitivity, and activate the peroxisome proliferator-activated gamma receptor. ACS Omega. 2024;9(5):5463–5484. doi: 10.1021/acsomega.3c07149
48. Li P, Zhang W, Jiang H, et al. Design, synthesis and biological evaluation of benzimidazole-rhodanine conjugates as potent topoisomerase II inhibitors. Medchemcomm. 2018;9(7):1194–1205. doi: 10.1039/c8md00278a
•• **This reference holds significant relevance in this study. It reports on the biological activity of rhodanine-containing non-nitroaromatic molecules. The authors have drawn upon the results from this reference to establish the rationale for the target conjugates on the hypothesis that they could possess antiparasitic activity as a result of dual mode of action.**
49. Zhu L, Ye C, Chen S, et al. Rhodanine derivatives containing 5-aryloxypyrazole moiety as anti-inflammatory and anticancer agents. Chem Biodivers. 2024;21(2):e202301844. doi: 10.1002/cbdv.202301844
50. Shepeta YL, Lozynskyi A, Tomkiv ZV, et al. Synthesis and evaluation of biological activity of rhodanine-pyrazoline hybrid molecules with 2-(2,6-dichlorophenylamino)-phenylacetamide fragment. Biopolym Cell. 2020;36(2):133–145. doi: 10.7124/bc.000A27
51. Nepali K, Lee HY, Liou JP. Nitro-group-containing drugs. J Med Chem. 2019;62(6):2851–2893. doi: 10.1021/acs.jmedchem.8b00147
•• **This reference holds significant relevance in this study. It highlights the important pharmacological role of the nitroaromatic group imparting several clinical drugs including antiparasitics with their actual the therapeutic effect. The authors have**

drawn upon the results from this reference to justify the incorporation of 5-nitroindole moiety as potential antiparasitic redox active pharmacophore.

52. Roldan MD, Perez-Reinado E, Castillo F, et al. Reduction of polynitroaromatic compounds: the bacterial nitroreductases. FEMS Microbiol Rev. 2008;32(3):474–500. doi: 10.1111/j.1574-6976.2008.00107.x
53. Hall BS, Bot C, Wilkinson SR. Nifurtimox activation by trypanosomal type I nitroreductases generates cytotoxic nitrile metabolites. J Biol Chem. 2011;286(15):13088–13095. doi: 10.1074/jbc.M111.230847
54. Wyllie S, Roberts AJ, Norval S, et al. Activation of bicyclic Nitro-drugs by a novel nitroreductase (NTR2) in Leishmania. PLOS Pathog. 2016;12(11):e1005971. doi: 10.1371/journal.ppat.1005971
55. de Morais-Teixeira E, Rabello A, Aguiar MMG. In vitro activity and in vivo efficacy of fexinidazole against new world leishmania species. J Antimicrob Chemother. 2019;74(8):2318–2325. doi: 10.1093/jac/dkz172

•• **This reference holds significant relevance in this study. The authors have drawn upon the results from this reference to formulate the hypothesis that the incorporation of 5-nitroindole, a nitroaromatic synthon like 5-nitroimidazole in fexinidazole, into the target compounds may impart them with enhanced antileishmanial activity.**

56. Patterson S, Wyllie S, Norval S, et al. The anti-tubercular drug delamanid as a potential oral treatment for visceral leishmaniasis. Elife. 2016;5:e09744. doi: 10.7554/eLife.09744
57. Van den Kerkhof M, Mabille D, Chatelain E, et al. In vitro and in vivo pharmacodynamics of three novel antileishmanial lead series. Int J Parasitol Drugs Drug Resist. 2018;8(1):81–86. doi: 10.1016/j.ijpddr.2018.01.006
58. Patterson S, Wyllie S, Stojanovski L, et al. The R enantiomer of the antitubercular drug PA-824 as a potential oral treatment for visceral leishmaniasis. Antimicrob Agents Chemother. 2013;57(10):4699–4706. doi: 10.1128/AAC.00722-13
59. Thompson AM, Marshall AJ, Maes L, et al. Assessment of a pretomanid analogue library for African trypanosomiasis: hit-to-lead studies on 6-substituted 2-nitro-6,7-dihydro-5H-imidazo[2,1-b][1,3]thiazine 8-oxides. Bioorg Med Chem Lett. 2018;28(2):207–213. doi: 10.1016/j.bmcl.2017.10.067
60. Reinhardt T, Lee KM, Niederegger L, et al. Indolin-2-one nitroimidazole antibiotics exhibit an unexpected dual mode of action. ACS Chem Biol. 2022;17(11):3077–3085. doi: 10.1021/acschembio.2c00462
61. Nimbarte VD, Wirmer-Bartoschek J, Gande SL, et al. Synthesis and in vitro evaluation of novel 5-nitroindole derivatives as c-myc G-Quadruplex binders with anticancer activity. ChemMedchem. 2021;16(10):1667–1679. doi: 10.1002/cmdc.202000835

•• **This reference holds significant relevance in this study. Authors have drawn upon the results from this reference to provide valuable assistance in the chemical synthesis of the target compounds.**

62. Bayindir S. A simple rhodanine-based fluorescent sensor for mercury and copper: the recognition of Hg2+ in aqueous solution and Hg2+/Cu2+ in organic solvent. J Photochem Photobiol A Chem. 2019;372:235–244. doi: 10.1016/j.jphotochem.2018.12.021
63. Daina A, Michielin O, Zoete V. SwissADME: a free web tool to evaluate pharmacokinetics, drug-likeness and medicinal chemistry friendliness of small molecules. Sci Rep. 2017;7:42717. doi: 10.1038/srep42717
64. Ndlovu K, Kannigadu C, Aucamp J, et al. Exploration of ethylene glycol linked nitrofurantoin derivatives against Leishmania: synthesis and in vitro activity. Arch Pharm (Weinheim). 2023;356(5):e2200529. doi: 10.1002/ardp.202200529
65. Zuma NH, Aucamp J, Viljoen M, et al. Synthesis, in vitro antileishmanial efficacy and hit/lead identification of nitrofurantoin-triazole hybrids. ChemMedchem. 2022;17(10):e202200023. doi: 10.1002/cmdc.202200023
66. Sechoaro K, Aucamp J, Kannigadu C, et al. Investigation of novel isatinylhydantoin derivatives as potential anti-kinetoplastid agents. ChemMedchem. 2025;20(1):e202400533. doi: 10.1002/cmdc.202400533
67. Siqueira-Neto JL, Song OR, Oh H, et al. Antileishmanial high-throughput drug screening reveals drug candidates with new scaffolds. PLOS Negl Trop Dis. 2010;4(5):e675. doi: 10.1371/journal.pntd.0000675
68. Kulshrestha A, Bhandari V, Mukhopadhyay R, et al. Validation of a simple resazurin-based promastigote assay for the routine monitoring of miltefosine susceptibility in clinical isolates of leishmania donovani. Parasitol Res. 2013;112(2):825–828. doi: 10.1007/s00436-012-3212-3
69. Jain SK, Sahu R, Walker LA, et al. A parasite rescue and transformation assay for antileishmanial screening against intracellular Leishmania donovani amastigotes in THP1 human acute monocytic leukemia cell line. J Vis Exp. 2012;30(70):4054. doi: 10.3791/4054
70. Njanpa CAN, Wouamba SCN, Yamthe LRT, et al. Bio-guided isolation of anti-leishmanial natural products from diospyros gracilescens L. (ebenaceae). BMC Complement Med Ther. 2021;21(1):106. doi: 10.1186/s12906-021-03279-1
71. Zuma NH, Aucamp J, Janse van Rensburg HD, et al. Synthesis and in vitro antileishmanial activity of alkylene-linked nitrofurantoin-triazole hybrids. Eur J Med Chem. 2023;246:115012. doi: 10.1016/j.ejmech.2022.115012
72. Hou T, Wang J, Zhang W, et al. ADME evaluation in drug discovery. 6. Can oral bioavailability in humans be effectively predicted by simple molecular property-based rules? J Chem Inf Model. 2007;47(2):460–463. doi: 10.1021/ci6003515
73. Ghose AK, Viswanadhan VN, Wendoloski JJ. A knowledge-based approach in designing combinatorial or medicinal chemistry libraries for drug discovery. 1. A qualitative and quantitative characterization of known drug databases. J Comb Chem. 1999;1(1):55–68. doi: 10.1021/cc9800071
74. Egan WJ, Merz KM Jr., Baldwin JJ. Prediction of drug absorption using multivariate statistics. J Med Chem. 2000;43(21):3867–3877. doi: 10.1021/jm000292e
75. Lipinski CA, Lombardo F, Dominy BW, et al. Experimental and computational approaches to estimate solubility and permeability in drug discovery and development settings. Adv Drug Deliv Rev. 2001;46(1–3):3–26. doi: 10.1016/s0169-409x(00)00129-0
76. Muegge I, Heald SL, Brittelli D. Simple selection criteria for drug-like chemical matter. J Med Chem. 2001;44(12):1841–1846. doi: 10.1021/jm015507e
77. Veber DF, Johnson SR, Cheng HY, et al. Molecular properties that influence the oral bioavailability of drug candidates. J Med Chem. 2002;45(12):2615–2623. doi: 10.1021/jm020017n
78. Hann MM, Keseru GM. Finding the sweet spot: the role of nature and nurture in medicinal chemistry. Nat Rev Drug Discov. 2012;11(5):355–365. doi: 10.1038/nrd3701
79. Teague SJ, Davis AM, Leeson PD, et al. The design of leadlike combinatorial libraries. Angew Chem Int Ed Engl. 1999;38(24):3743–3748. doi: 10.1002/(SICI)1521-3773(19991216)38:24<3743:AID-ANIE3743>3.0.CO;2-U
80. Goodwin JJ. Rationale and benefit of using high throughput solubility screens in drug discovery. Drug Discov Today Technol. 2006;3(1):67–71. doi: 10.1016/j.ddtec.2005.03.001
81. Katsuno K, Burrows JN, Duncan K, et al. Hit and lead criteria in drug discovery for infectious diseases of the developing world. Nat Rev Drug Discov. 2015;14(11):751–758. doi: 10.1038/nrd4683
82. Daina A, Zoete V. A BOILED-Egg to predict gastrointestinal absorption and brain penetration of small molecules. ChemMedchem. 2016;11(11):1117–1121. doi: 10.1002/cmdc.201600182
83. Saunders EC, Ng WW, Kloehn J, et al. Induction of a stringent metabolic response in intracellular stages of Leishmania mexicana leads to increased dependence on mitochondrial metabolism. PLOS Pathog. 2014;10(1):e1003888. doi: 10.1371/journal.ppat.1003888
84. Zulfiqar B, Shelper TB, Avery VM. Leishmaniasis drug discovery: recent progress and challenges in assay development. Drug Discov Today. 2017;22(10):1516–1531. doi: 10.1016/j.drudis.2017.06.004
85. De Muylder G, Vanhollebeke B, Caljon G, et al. Naloxonazine, An amastigote-specific compound, affects leishmania parasites through modulation of host-encoded functions. PLOS Negl Trop Dis. 2016;10(12):e0005234. doi: 10.1371/journal.pntd.0001253

86. Liu S, Su M, Song SJ, et al. Marine-derived penicillium species as producers of cytotoxic metabolites. Mar Drugs. 2017;15(10):329. doi: 10.3390/md15100329
87. Fu J, Chen H, Soroka DN, et al. Cysteine-conjugated metabolites of ginger components, shogaols, induce apoptosis through oxidative stress-mediated p53 pathway in human colon cancer cells. J Agric Food Chem. 2014;62:4632–4642. doi: 10.1021/jf501351r
88. Finiuk NS, Hreniuh VP, Ostapiuk YV, et al. Antineoplastic activity of novel thiazole derivatives. Biopolym Cell. 2017;33(2):135–146. doi: 10.7124/bc.00094B